

Modern Computational Methodologies for new glass development

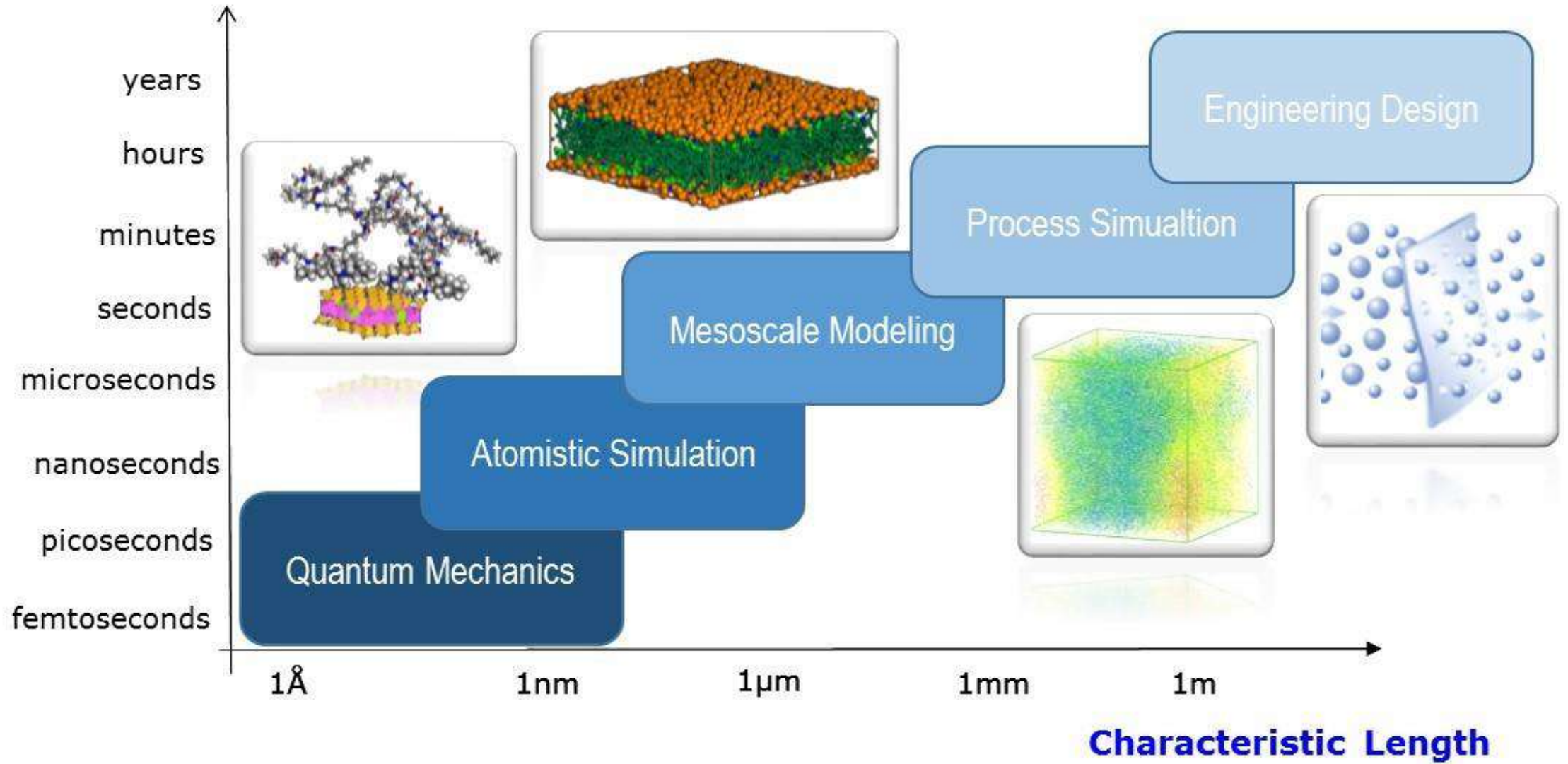
Alfonso Pedone

Department of Chemical and Geological Sciences
University of Modena and Reggio Emilia

Outline of the Lecture

- **Computational Methods to Simulate Glasses**
 - Molecular Dynamics Simulations (Born-Oppenheimer, Carr-Parrinello, classical)
 - Density Functional Theory
 - Empirical Force-Fields
 - Machine Learning Potentials
- **Validation of Glass Structures**
- **Ab initio MD and DFT: when are mandatory**
- **Performance of Empirical and ML-potentials: Sodium Silicate Glasses and Mixed Alkali Effect in Aluminosilicate Glasses**
- **Mechanical Properties: tensile, compression and indentation tests**
- **The timescale problem: studying Crystallization through Metadynamics Simulations**
- **Conclusions**

Characteristic Time

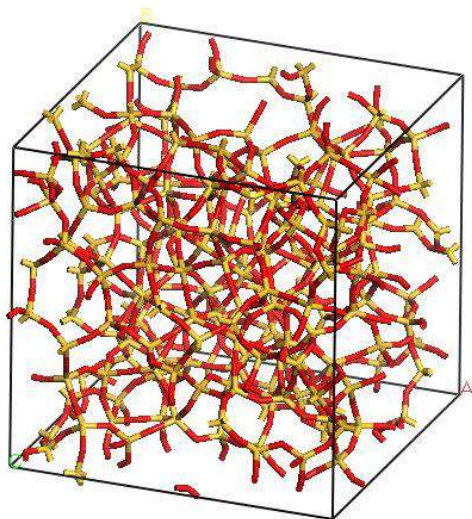


Molecular Dynamics Simulations

The classical equations of motion (Newton II law) are integrated numerically

$$\frac{\partial^2 \mathbf{r}_i}{\partial t^2} = \frac{\mathbf{F}_i}{m_i} = -\frac{\nabla_i U(\mathbf{r})}{m_i}$$

Trajectory: positions, velocities and accelerations of atoms in time



Potential Energy Surface

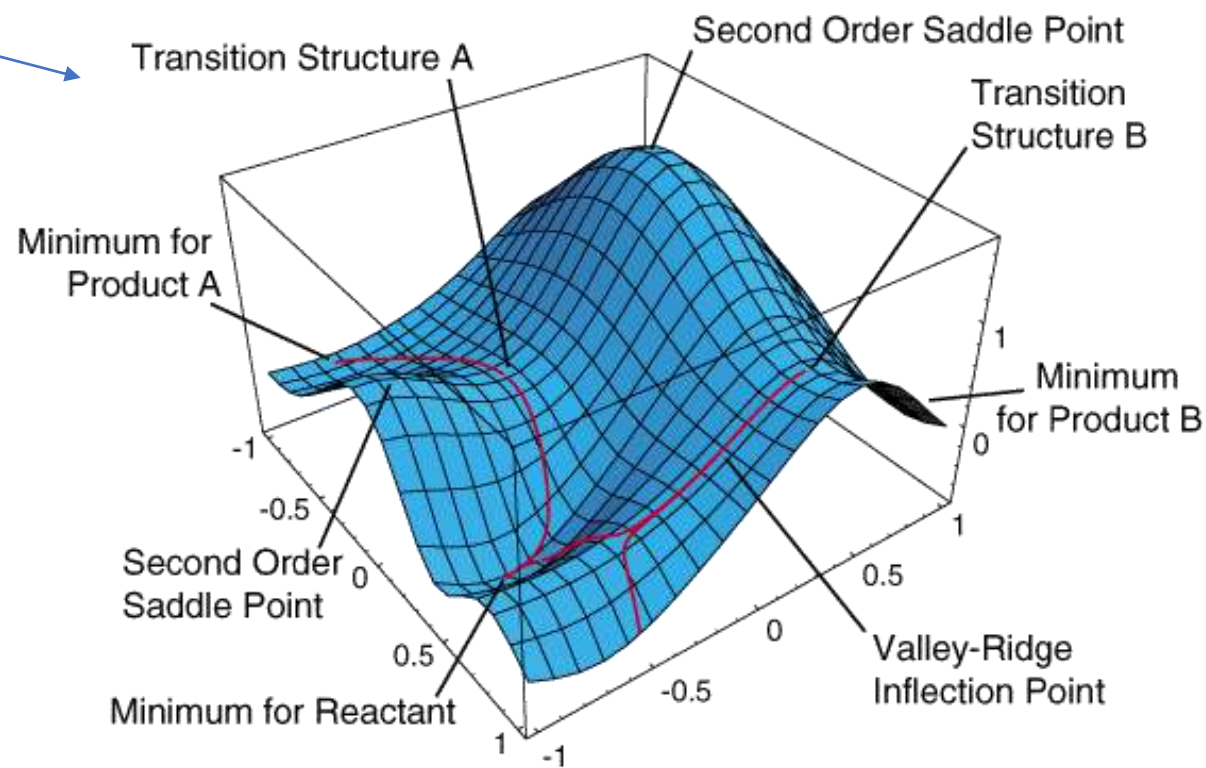
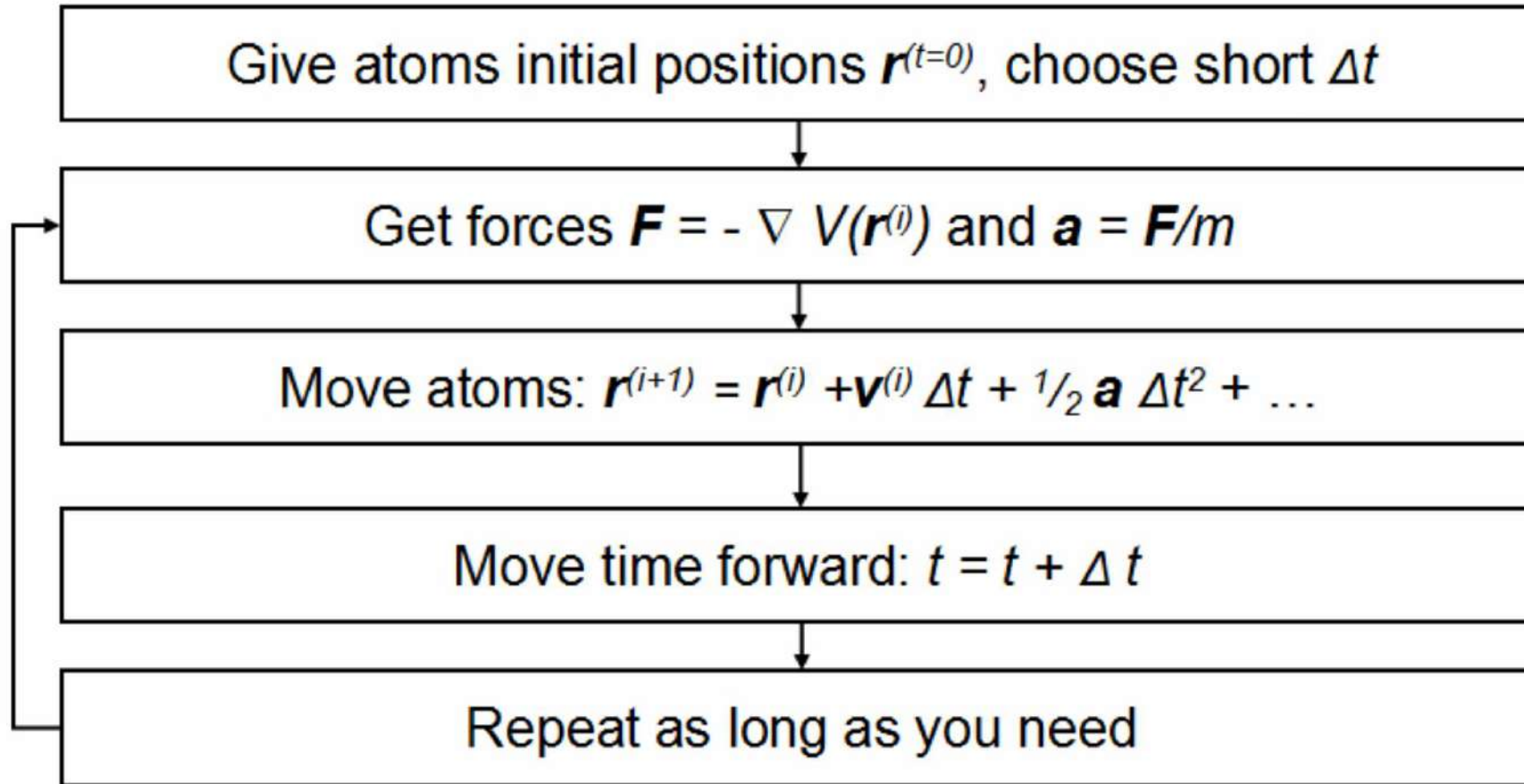


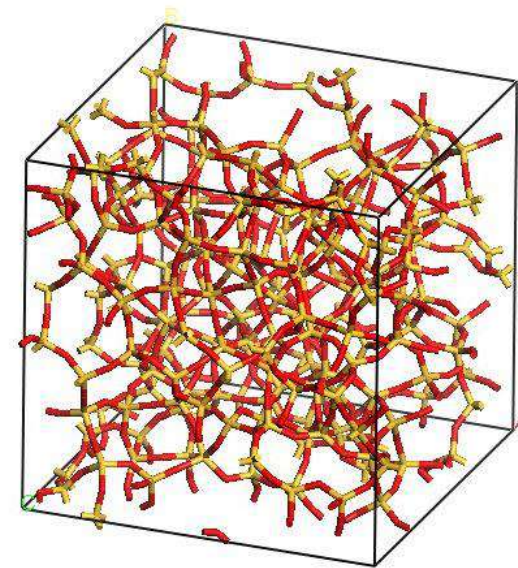
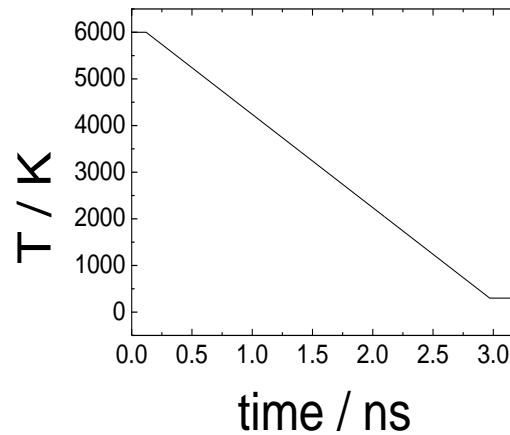
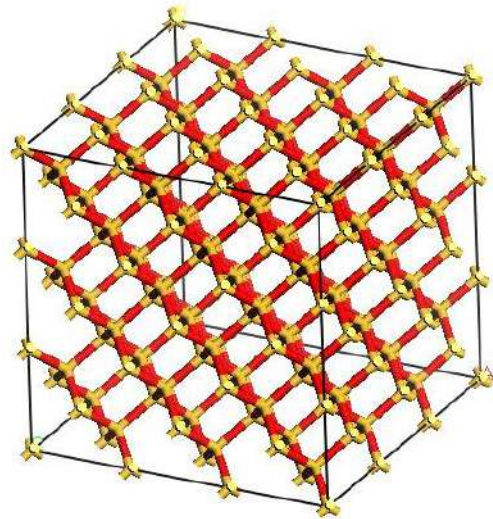
(Image taken from <http://www.chem.wayne.edu/~hbs/chm6440/PES.gif>)

Scheme of a basic classical MD algorithm



Exploiting MD simulations to generate Glass Structures

- Simulated glass structures are prepared computationally in the same way as real glasses.
- Models of crystalline (or random) systems are melted; the melts are then quenched, freezing the structure into a disordered glassy phase.



- Quenching rates much higher than the experimental ones ($0.5-5 \cdot 10^{12}$ K/s vs 1-100 K/s)
- The fictive temperature of the simulated glass is higher than the target temperature
- More disordered structure than the real ones

Molecular Dynamics Simulations

$$m \frac{d^2 \mathbf{R}}{dt^2} = -\nabla U(\mathbf{R})$$

Classical MD

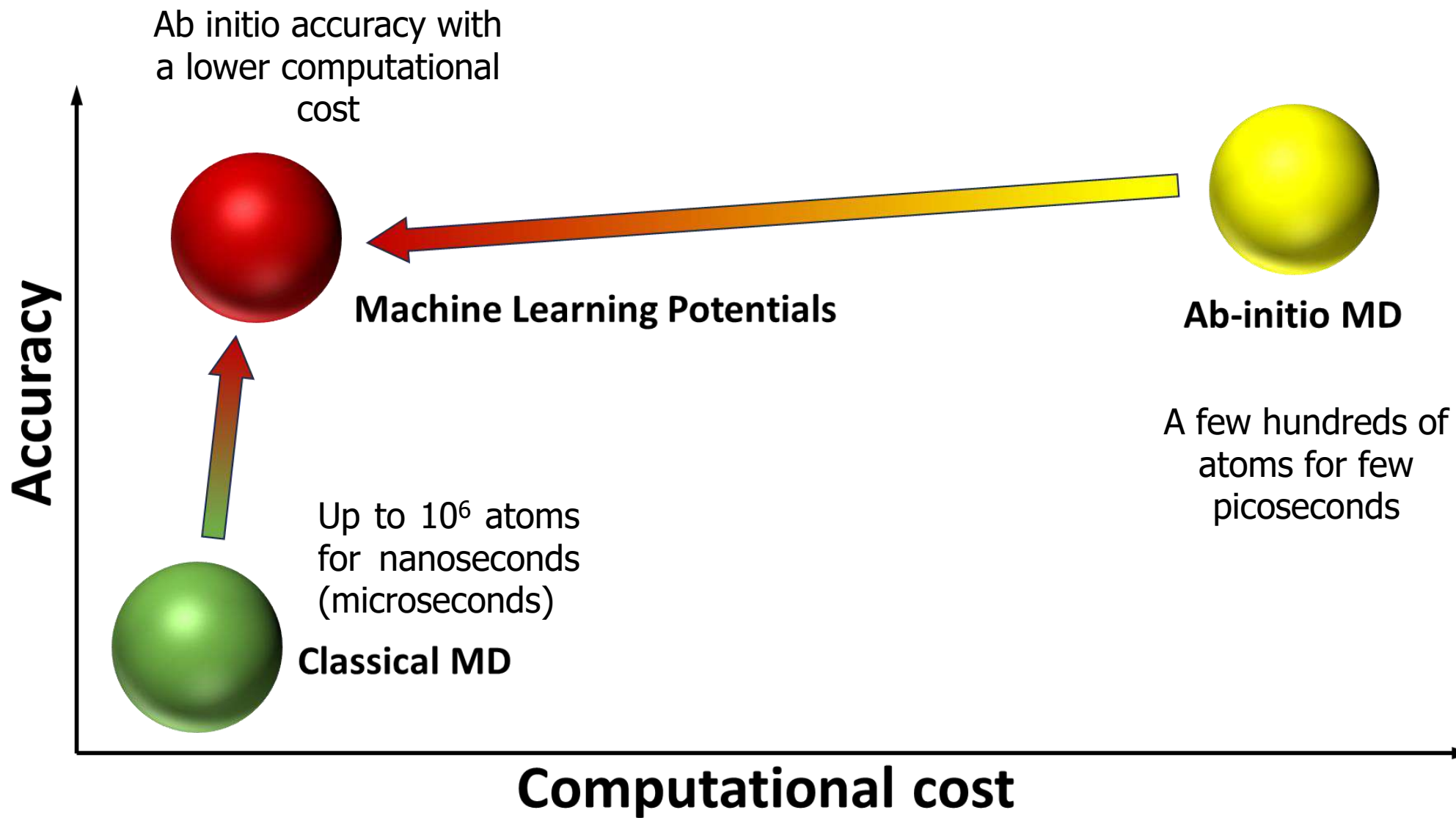
The PES is described by empirical parametric functions of nuclear (internal coordinates) (Force-Fields)

ML-accelerated MD

PES is described by ML algorithms

Ab initio MD
Born-Oppeneimer MD
Carr-Parrinello MD

PES computed at the Density Functional Theory level



Density Functional Theory (DFT): basics



Hohenberg-Kohn and Kohn-Sham (1964) established the rules of the **DFT** (Density Functional Theory) to compute the ground state energy as a **functional** of the electron density

Based on 2 Theorems:

- **Theorem 1.** The external potential or the ground state energy E of a molecular system is a unique functional of electron density.

$$E = E[\rho(r)]$$

- **Theorem 2.** The electron density that minimizes the energy of the overall functional is the true ground state electron density
- $E[\rho(r)] \geq E_0[\rho_0(r)]$

KOHN-SHAM FORMULATION

$$\rho(\mathbf{x}) = \sum_{i=1}^{N^{occ}} f_i |\psi_i(\mathbf{x})|^2$$

single-particle wavefunctions $\psi_i(\mathbf{x})$ are used to express the electron density

f_i are the occupation numbers (1 – spin unrestricted ; 2 – spin restricted)

$$\int \psi_i^*(\mathbf{x}) \psi_j(\mathbf{x}) d^3x = \delta_{ij}$$

the wavefunctions are subjected to the orthonormality constraint

KS DFT total energy is written as

$$E^{KS}[\{\psi_i\}] = E_k[\{\psi_i\}] + E_H[\rho] + E_{xc}[\rho] + E_{eI}[\rho] + E_{II}$$

Electron-nuclei interactions

Electron-electron interactions

Nuclei-nuclei interactions

Jacob's ladder of XC functionals

$$E_k[\{\psi_i\}] = \sum_{i=1}^{N^{occ}} f_i \int \psi_i^*(\mathbf{x}) \left(-\frac{1}{2} \nabla^2 \right) \psi_i(\mathbf{x}) d^3x$$

Schrödinger-like kinetic energy expressed in terms of the single particle wavefunctions

$$E_H[\rho] = \frac{1}{2} \iint \frac{\rho(\mathbf{x})\rho(\mathbf{y})}{|\mathbf{x}-\mathbf{y}|} d^3x d^3y$$

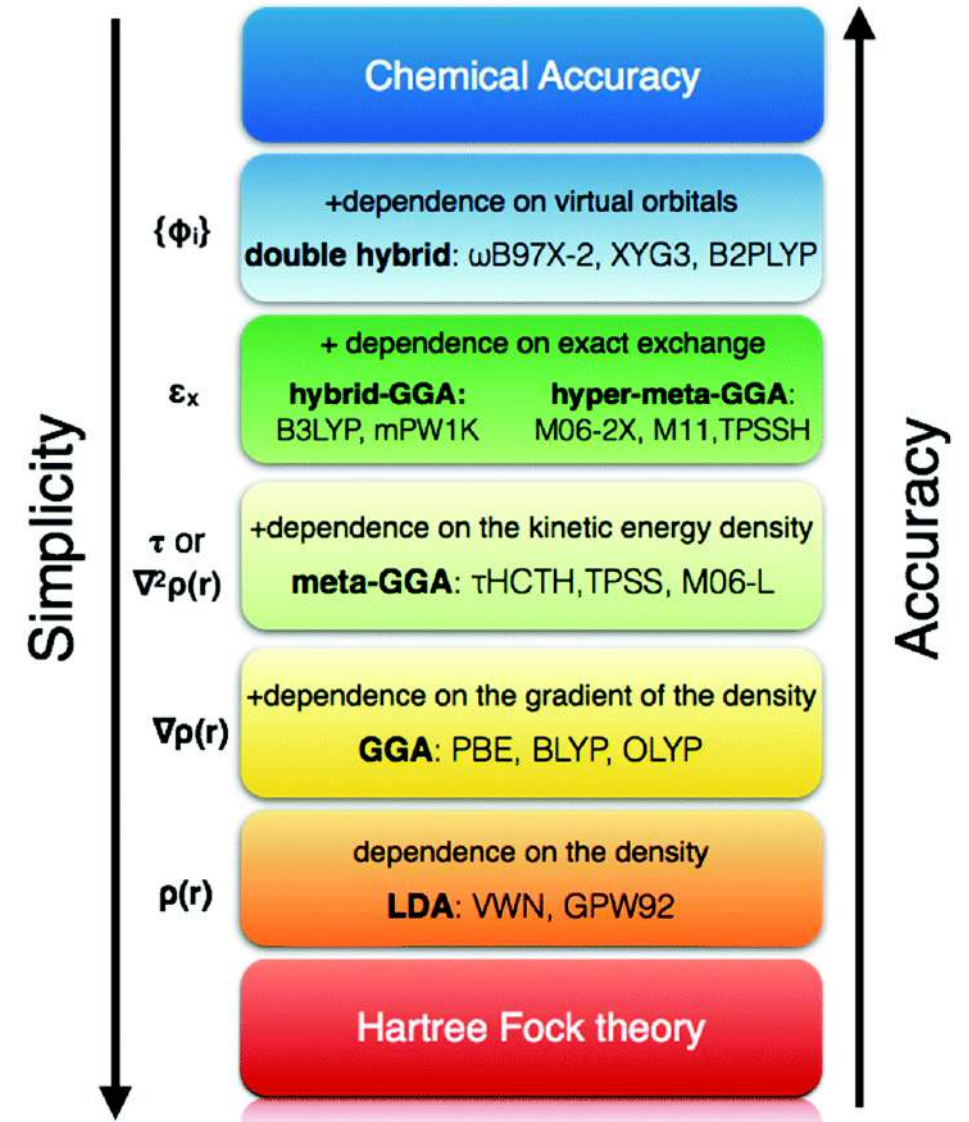
Hartree energy, i.e. the Coulomb electrostatic interaction between two charge distributions

$$E_{el}[\rho] = - \int \sum_{I=1}^M \frac{Z_I \rho(\mathbf{x})}{|\mathbf{x}-\mathbf{R}_I|} d^3x$$

electrostatic interaction between electrons and nuclei

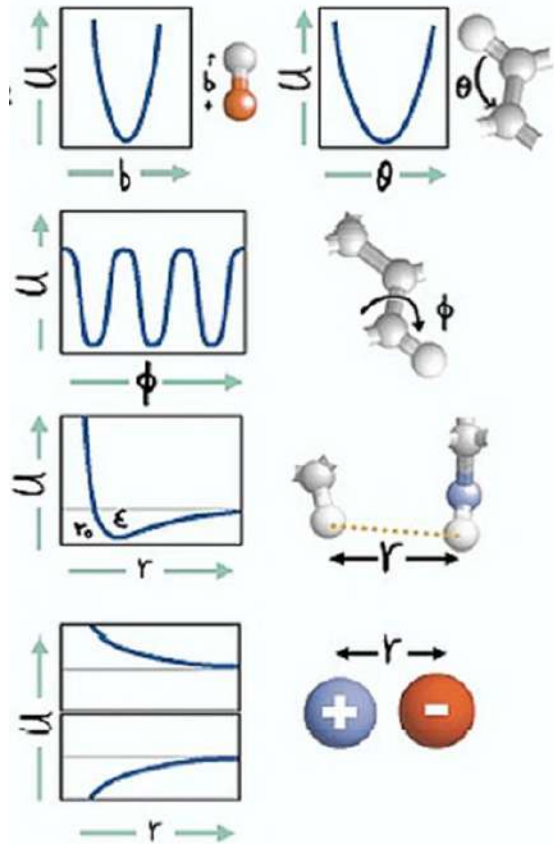
$$E_{xc}[\rho] = ? \quad \text{Exact Functional Unknown}$$

exchange interaction and the electron correlations due to many body effects

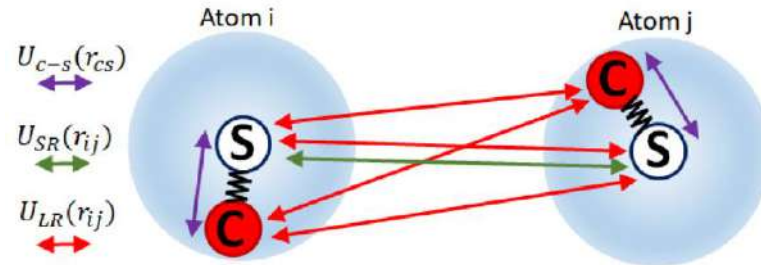


Force-Fields for Silica-based Glasses: our experience

Rigid Ionic Model

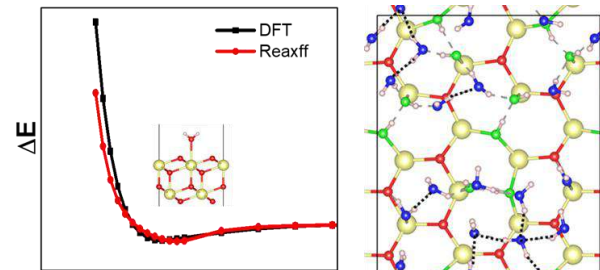


Core Shell Model

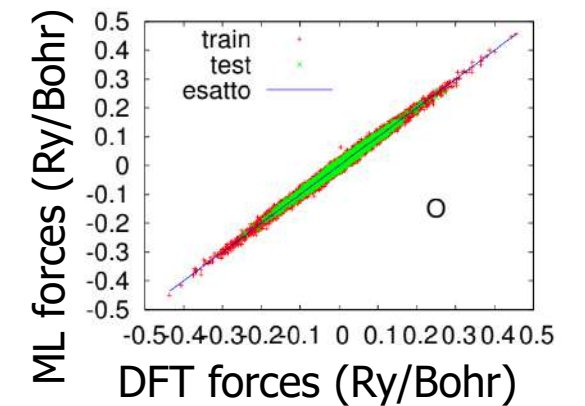
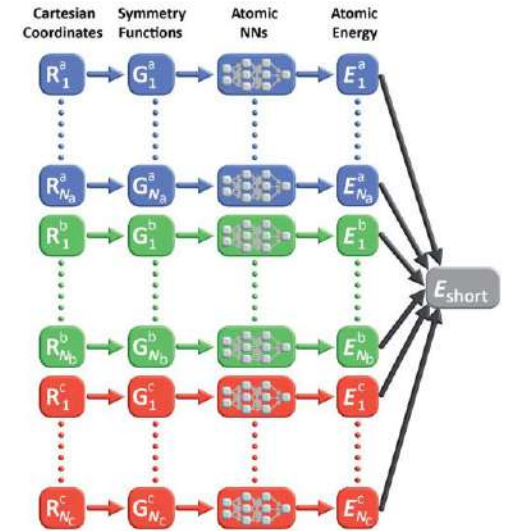


ReaxFF

$$E_{\text{tot}} = E_{\text{bond}} + E_{\text{val}} + E_{\text{tors}} + E_{\text{over}} + E_{\text{under}} + E_{\text{lp}} + E_{\text{vdwals}} + E_{\text{coulomb}}$$



ML-FFs



A New Self-Consistent Empirical Interatomic Potential Model for Oxides, Silicates, and Silica-Based Glasses

Alfonso Pedone,[†] Gianluca Malavasi,[†] M. Cristina Menziani,[†] Alastair N. Cormack,[‡] and Ulderico Segre^{*†}

Improved empirical force field for multicomponent oxide glasses and crystals

Marco Bertani[✉], Maria Cristina Menziani[✉], and Alfonso Pedone[✉]

Department of Chemical and Geological Sciences, University of Modena and Reggio Emilia, via G. Campi 103, 41125 Modena, Italy

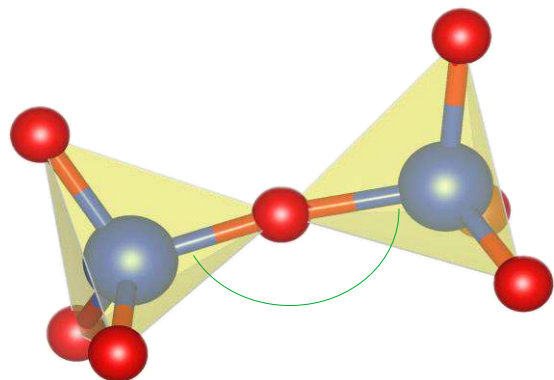
PMMCS

$$U_{ij} = \frac{z_i z_j e^2}{r_{ij}} + D_{ij} \left(\left\{ 1 - \exp \left[-a_{ij} (r_{ij} - r_{ij}^0) \right] \right\}^2 - 1 \right) + \frac{B_{ij}}{r_{ij}^{12}}$$

Coulomb

Morse function:
Short term (VdW)
interactions

Repulsive
(high T and P)



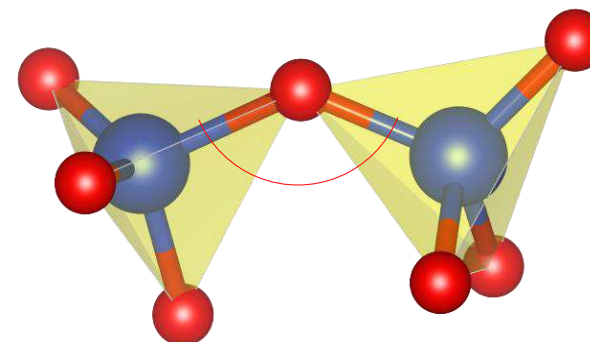
Repulsive interaction

$$U(r_{ij}) = A_{ij} \cdot e^{-\frac{r_{ij}}{\rho_{ij}}}$$

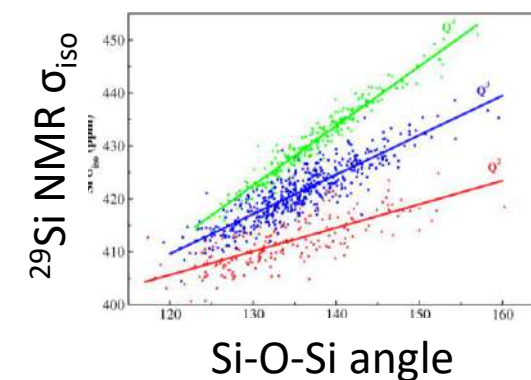
Three-body screened harmonic

$$U(\theta_{ijk}) = \frac{K_{ijk}}{2} (\theta_{ijk} - \theta_0)^2 \cdot e^{-\left(\frac{r_{ij}}{\rho_{ij}} - \frac{r_{jk}}{\rho_{jk}}\right)}$$

BMP



M. Bertani
UNIMORE



Elements Covered by our FFs

1 H Hydrogen																	2 He Helium
3 Li Lithium	4 Be Beryllium											5 B Boron	6 C Carbon	7 N Nitrogen	8 O Oxygen	9 F Fluorine	10 Ne Neon
11 Na Sodium	12 Mg Magnesium											13 Al Aluminium	14 Si Silicon	15 P Phosphorus	16 S Sulfur	17 Cl Chlorine	18 Ar Argon
19 K Potassium	20 Ca Calcium	21 Sc Scandium	22 Ti Titanium	23 V Vanadium	24 Cr Chromium	25 Mn Manganese	26 Fe Iron	27 Co Cobalt	28 Ni Nickel	29 Cu Copper	30 Zn Zinc	31 Ga Gallium	32 Ge Germanium	33 As Arsenic	34 Se Selenium	35 Br Bromine	36 Kr Krypton
37 Rb Rubidium	38 Sr Strontium	39 Y Yttrium	40 Zr Zirconium	41 Nb Niobium	42 Mo Molybdenum	43 Tc Technetium	44 Ru Ruthenium	45 Rh Rhodium	46 Pd Palladium	47 Ag Silver	48 Cd Cadmium	49 In Indium	50 Sn Tin	51 Sb Antimony	52 Te Tellurium	53 I Iodine	54 Xe Xenon
55 Cs Caesium	56 Ba Barium	57 La Lanthanum	72 Hf Hafnium	73 Ta Tantalum	74 W Tungsten	75 Re Rhenium	76 Os Osmium	77 Ir Iridium	78 Pt Platinum	79 Au Gold	80 Hg Mercury	81 Tl Thallium	82 Pb Lead	83 Bi Bismuth	84 Po Polonium	85 At Astatine	86 Rn Radon
87 Fr Francium	88 Ra Radium	89 Ac Actinium	104 Rf Rutherfordium	105 Db Dubnium	106 Sg Seaborgium	107 Bh Bohrium	108 Hs Hassium	109 Mt Meitnerium	110 Ds Darmstadtium	111 Rg Roentgenium	112 Cn Copernicium	113 Nh Nihonium	114 Fl Flerovium	115 Mc Moscovium	116 Lv Livermorium	117 Ts Tennessine	118 Og Oganesson

* 58 Ce Cerium	59 Pr Praseodymium	60 Nd Neodymium	61 Pm Promethium	62 Sm Samarium	63 Eu Europium	64 Gd Gadolinium	65 Tb Terbium	66 Dy Dysprosium	67 Ho Holmium	68 Er Erbium	69 Tm Thulium	70 Yb Ytterbium	71 Lu Lutetium
** 90 Th Thorium	91 Pa Protactinium	92 U Uranium	93 Np Neptunium	94 Pu Plutonium	95 Am Americium	96 Cm Curium	97 Bk Berkelium	98 Cf Californium	99 Es Einsteinium	100 Fm Fermium	101 Md Mendelevium	102 No Nobelium	103 Lr Lawrencium

- Silicates (Si-O-Si, Si-Si)
- Aluminosilicates (Al-Si, Al-Al)
- Phosphates (P-O-P, P-P)
- Phosphosilicates (P-O-Si, P-Si)
- Borates (B-O*, B-O-B, B-B)
- Borosilicates (B-O*, B-O-Si, B-Si)



PMMCS



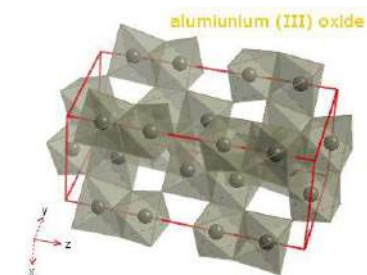
BMP only



BMP & PMMCS

Fitting Strategy

PMMCS: Empirical Fitting on Structure and Elastic constants of binary oxide crystals



BMP: Empirical fitting on T-O-T angles and densities of crystals

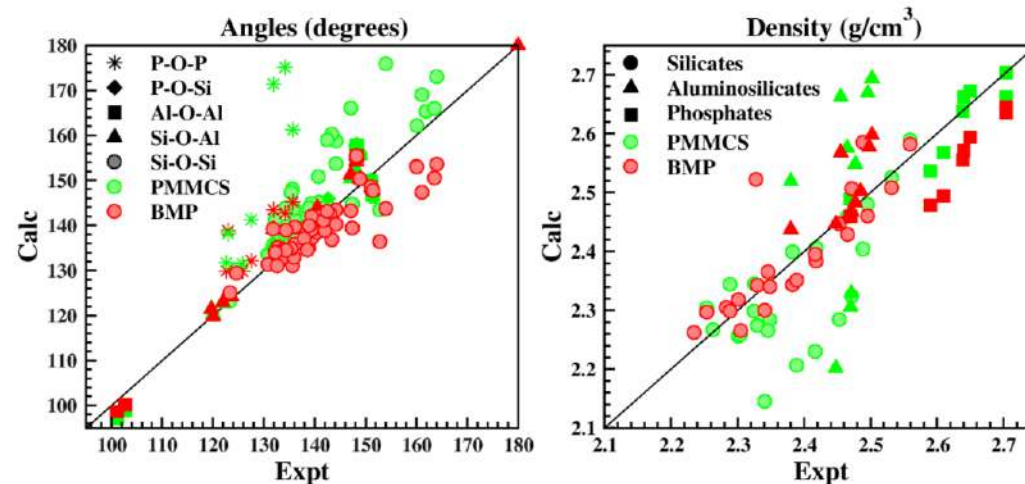
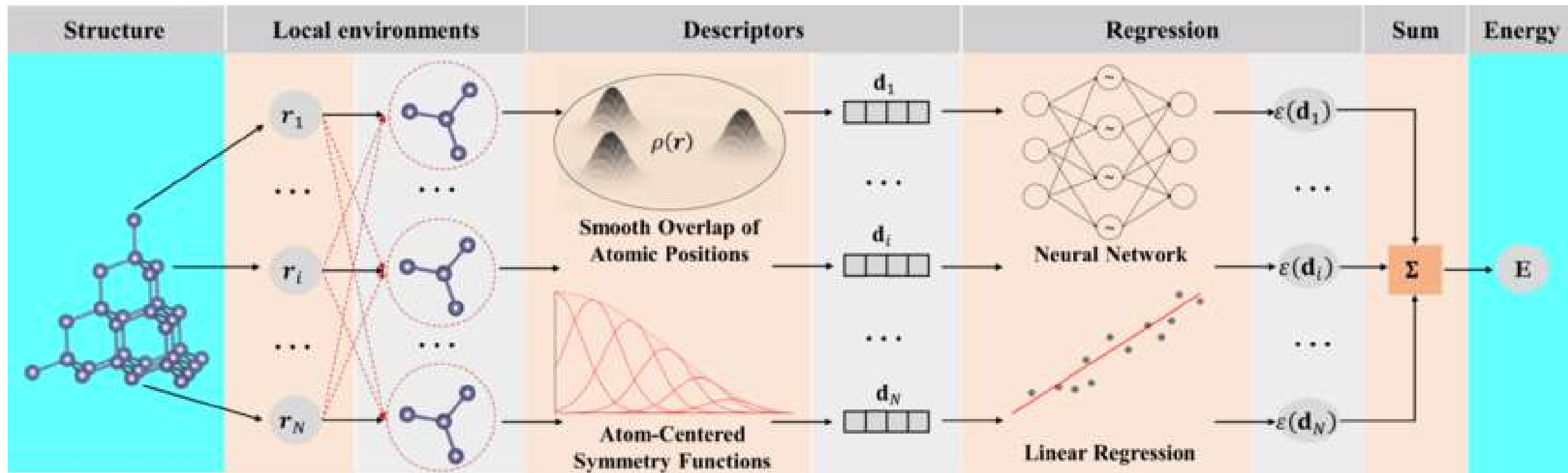
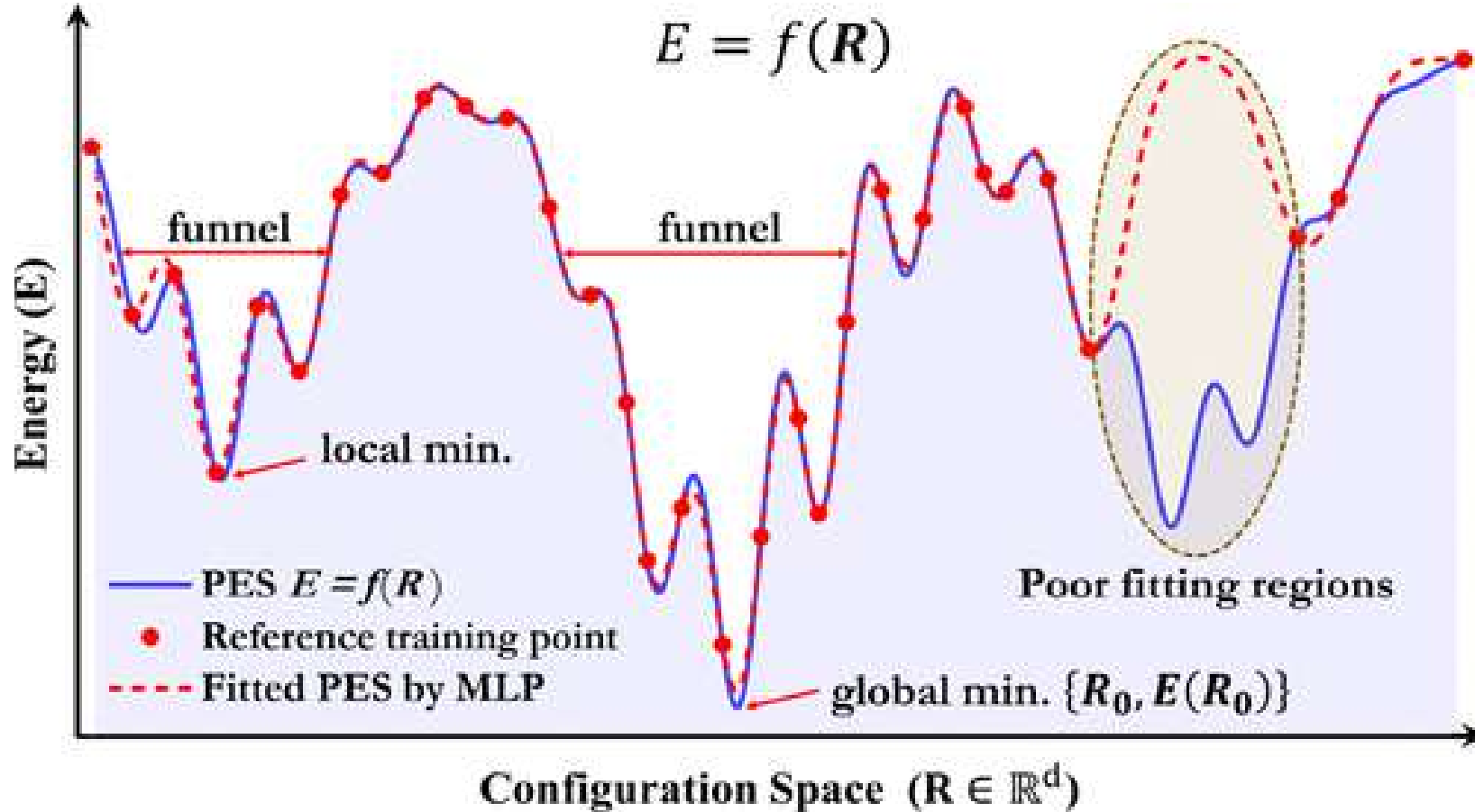


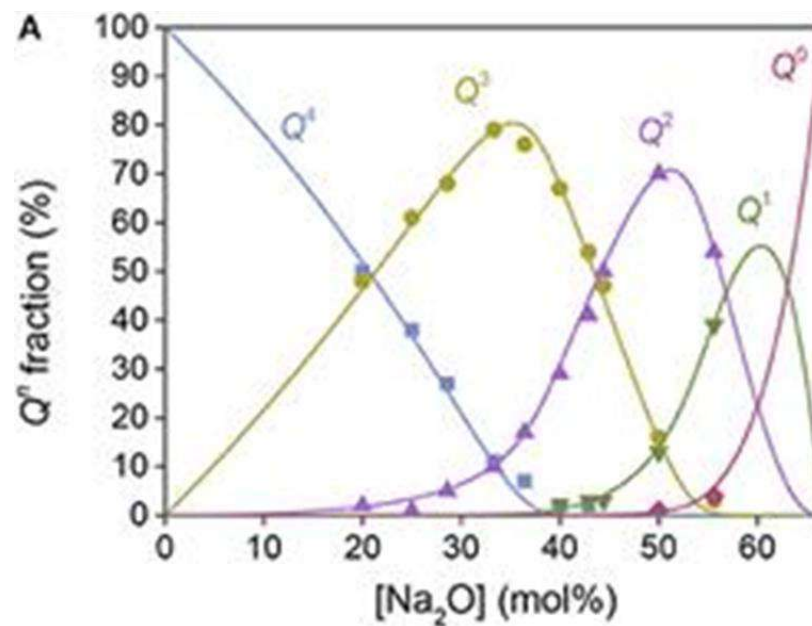
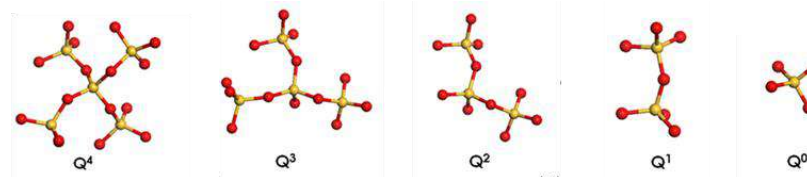
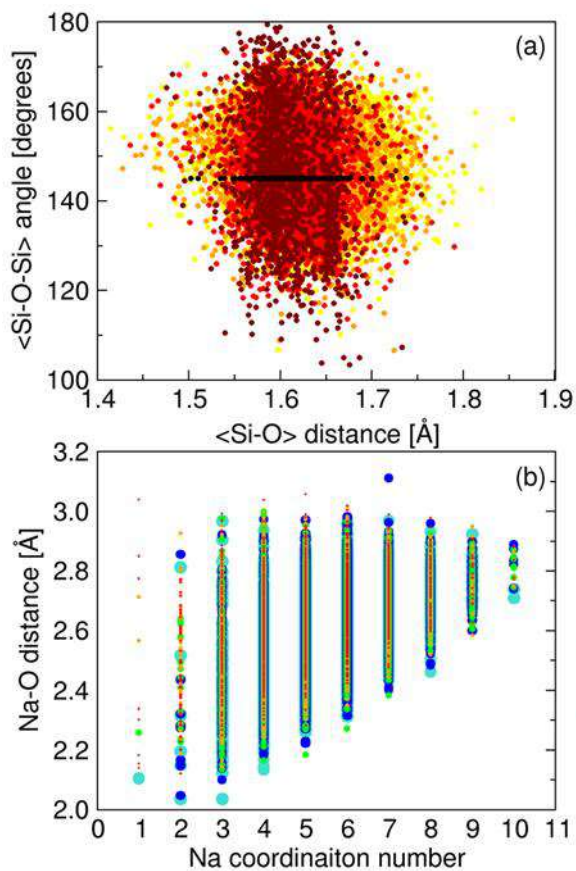
Illustration of descriptor-based machine learning potentials.





ML techniques are not extrapolative so your dataset must contain all possible configurations that you can encounter during MD simulations

Problems with the generation of a dataset for oxide glasses



The dimensionality of the configurational and compositional space in multicomponent oxide glasses is enormous!

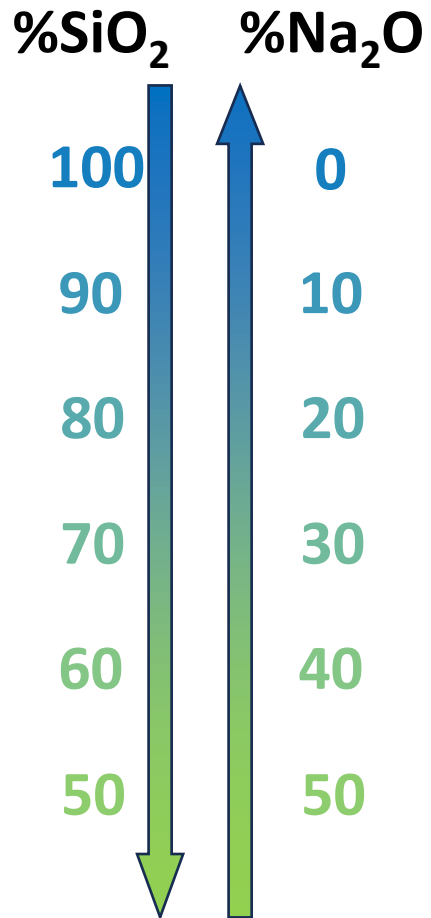
ML Potentials for Sodium Silicate Glasses: Dataset Generation

Composition

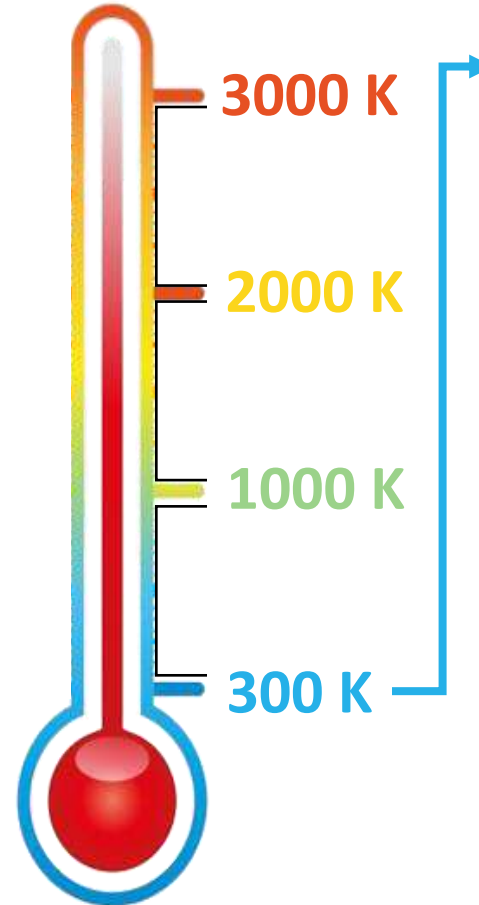
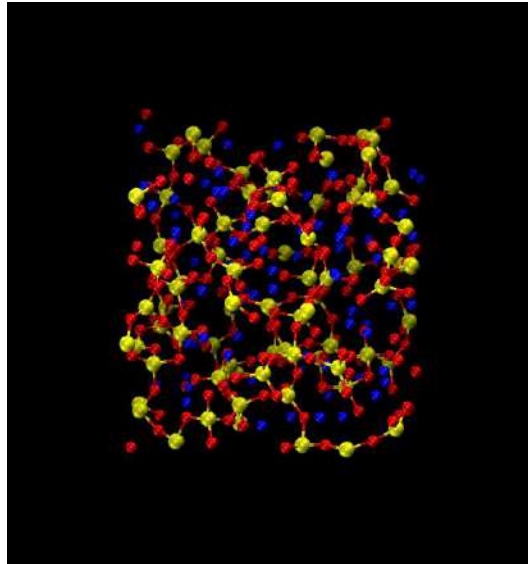
MD simulations

Temperature

Modifications



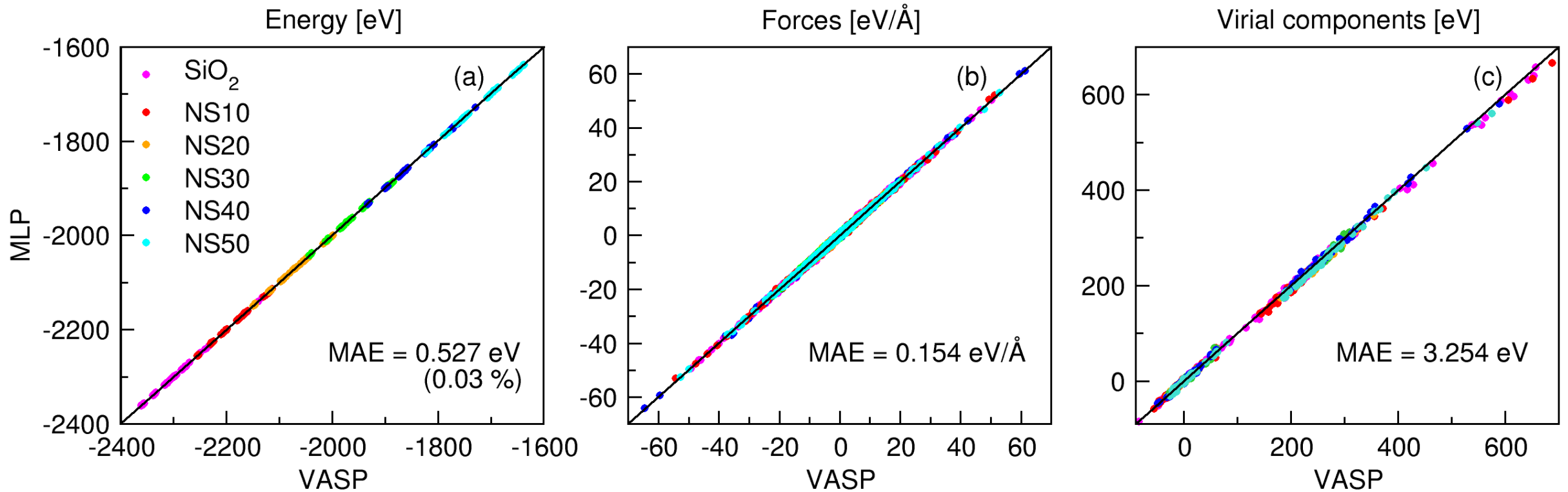
20 simulations for each composition (300 atoms)



½ DFT optimized (PBE)
½ Random distortion

TOTAL

1080 structures
324000 atoms



Scatter plot for (a) total energies, (b) forces on the x, y, and z, and (c) virials computed at the DFT level and predicted by the MLP for the test set.

Validating the glass structural models

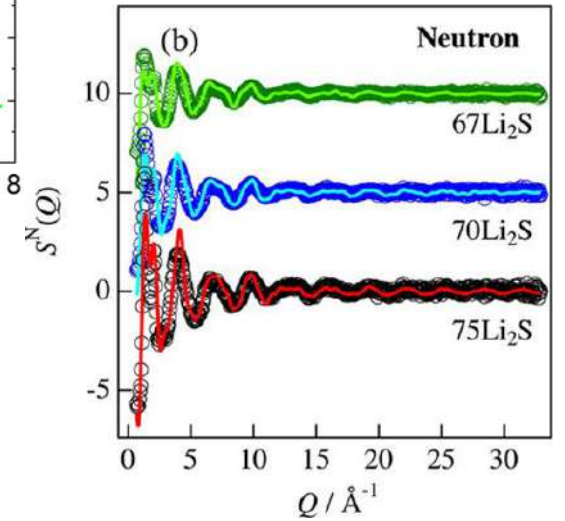
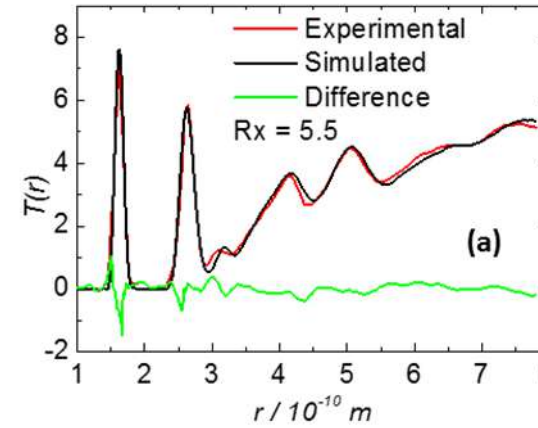
Real Space Correlation Functions

Neutron & X-Ray Structure Factors

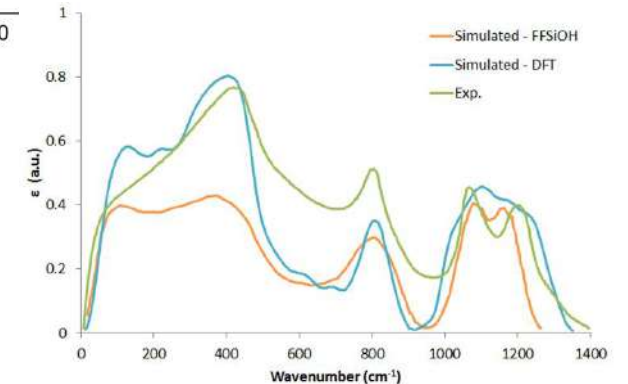
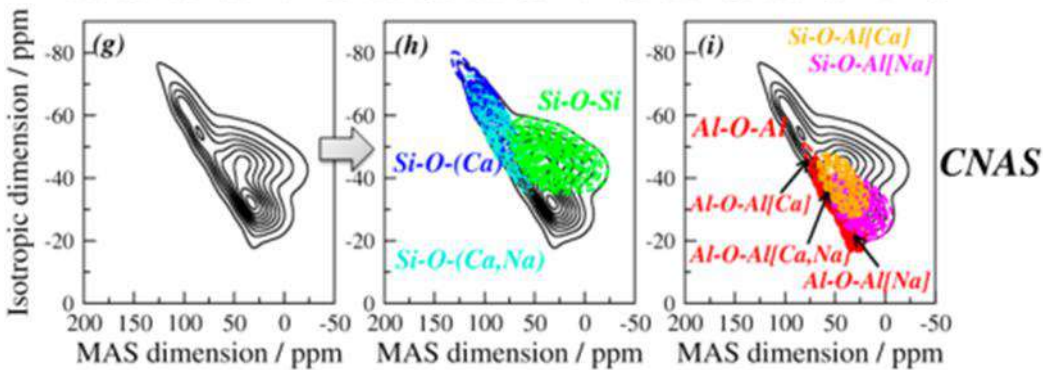
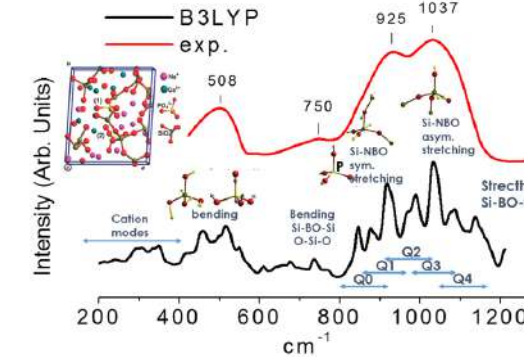
IR & RAMAN Spectroscopy

Phonon Dispersion Spectra

NMR Spectroscopy

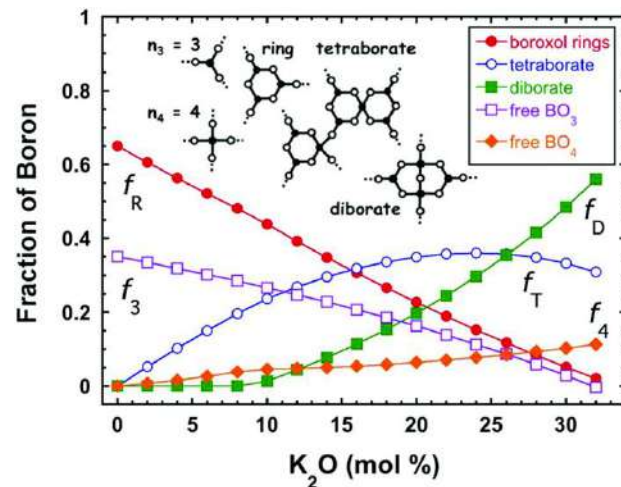


IR SPECTRA 45S5 Bioglass®

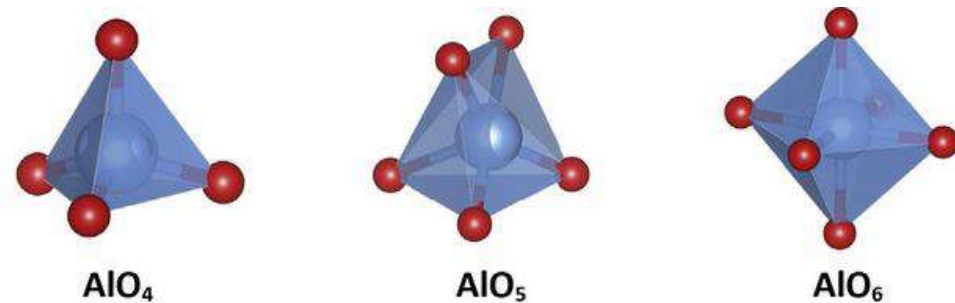


AI MD simulations: when it is mandatory

- When we want accurate and reliable results
- Reactivity
- For studying complex systems for which empirical force fields are not available or accurate (systems containing elements whose coordination changes with composition or it is difficult to reproduce because quantum mechanical effects are important, i.e. Jahn Teller effect).



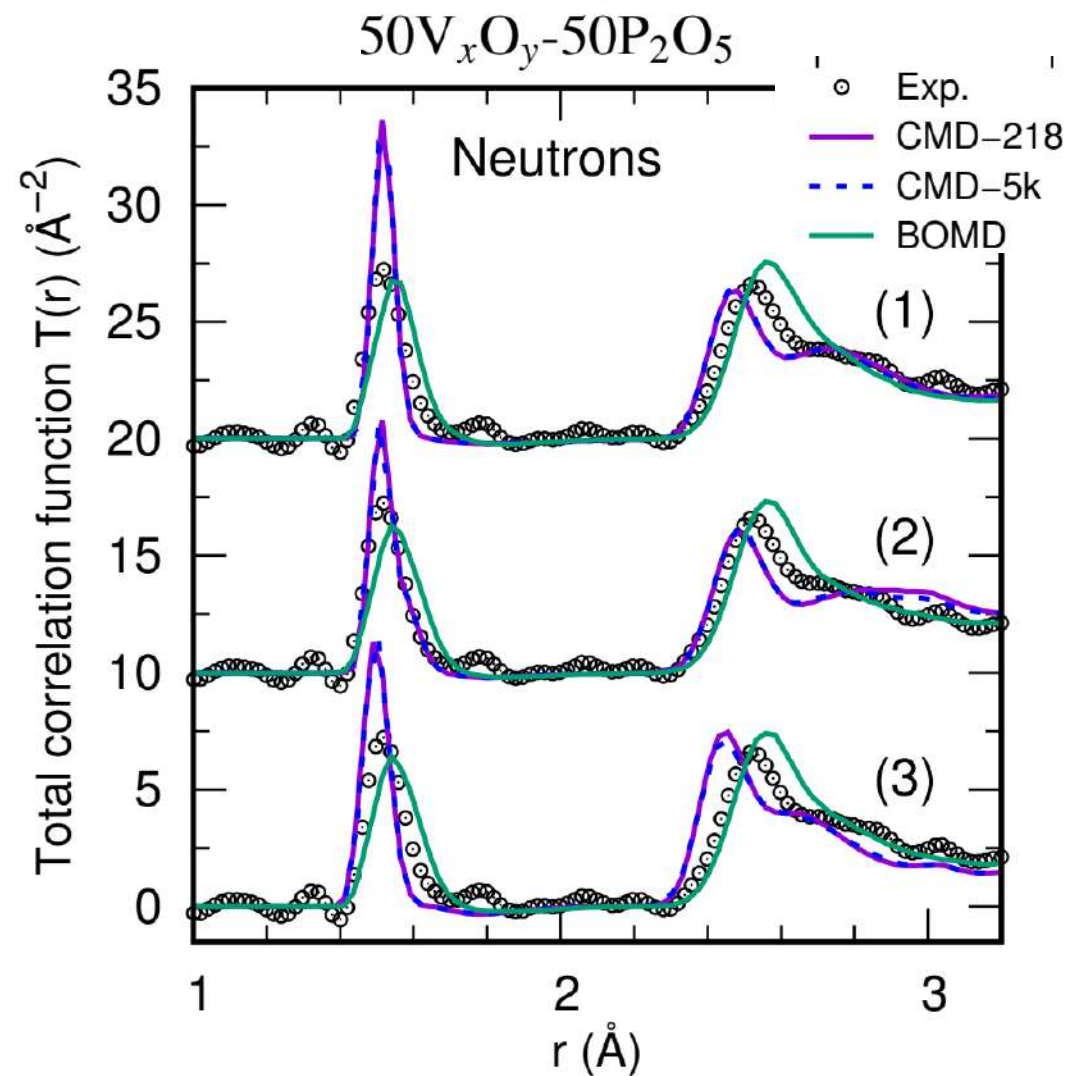
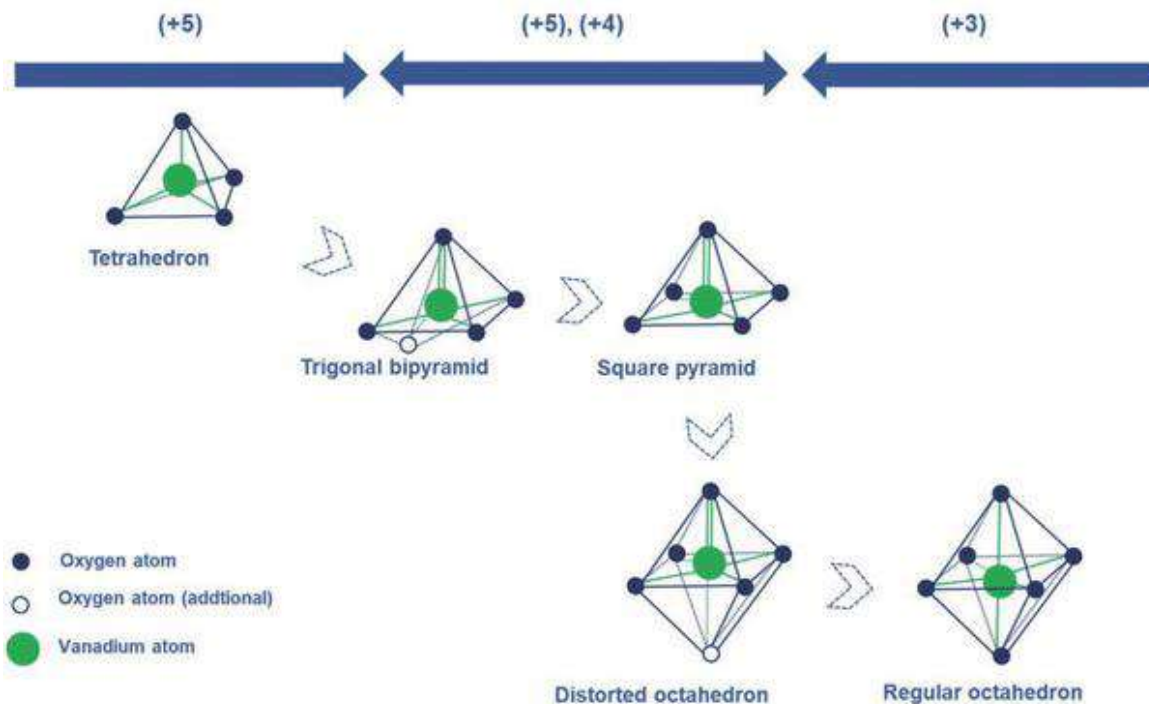
Boron-containing glasses



Aluminosilicate Glasses with peraluminous composition

Glasses containing transition metal elements: i.e. Vanadium

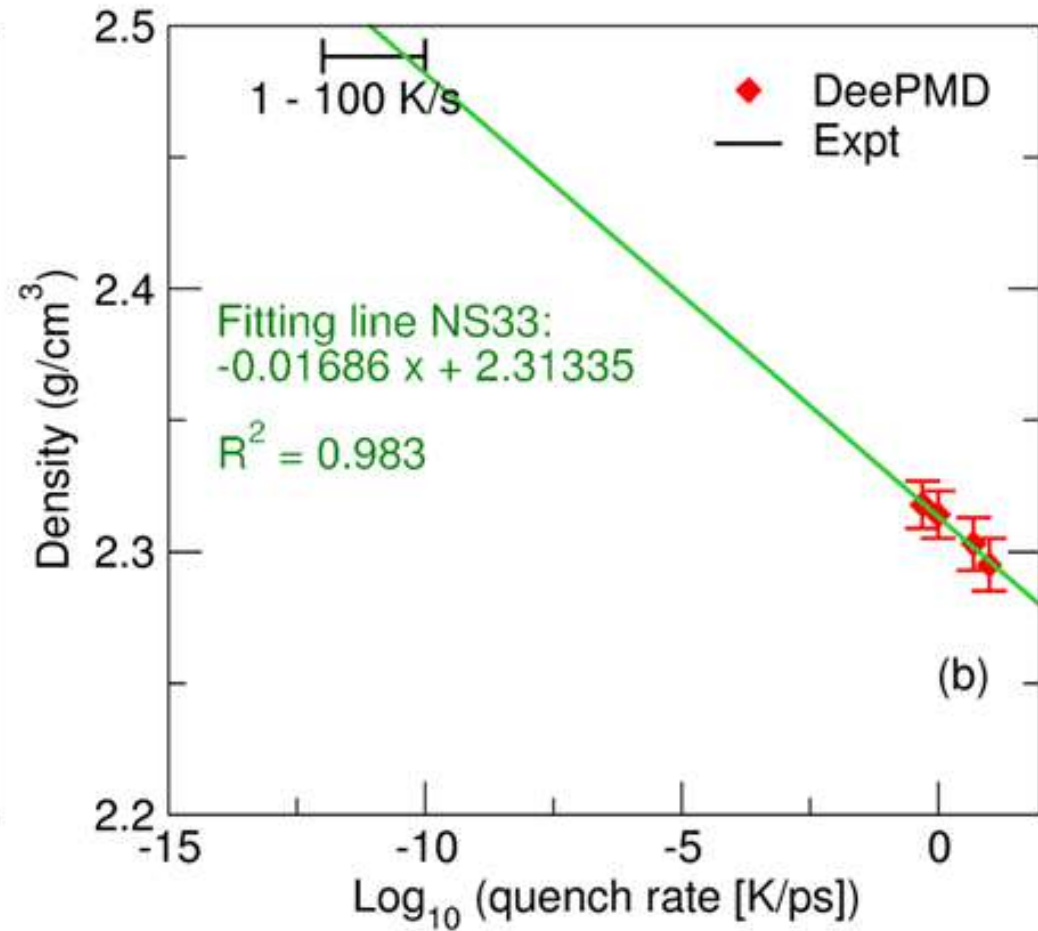
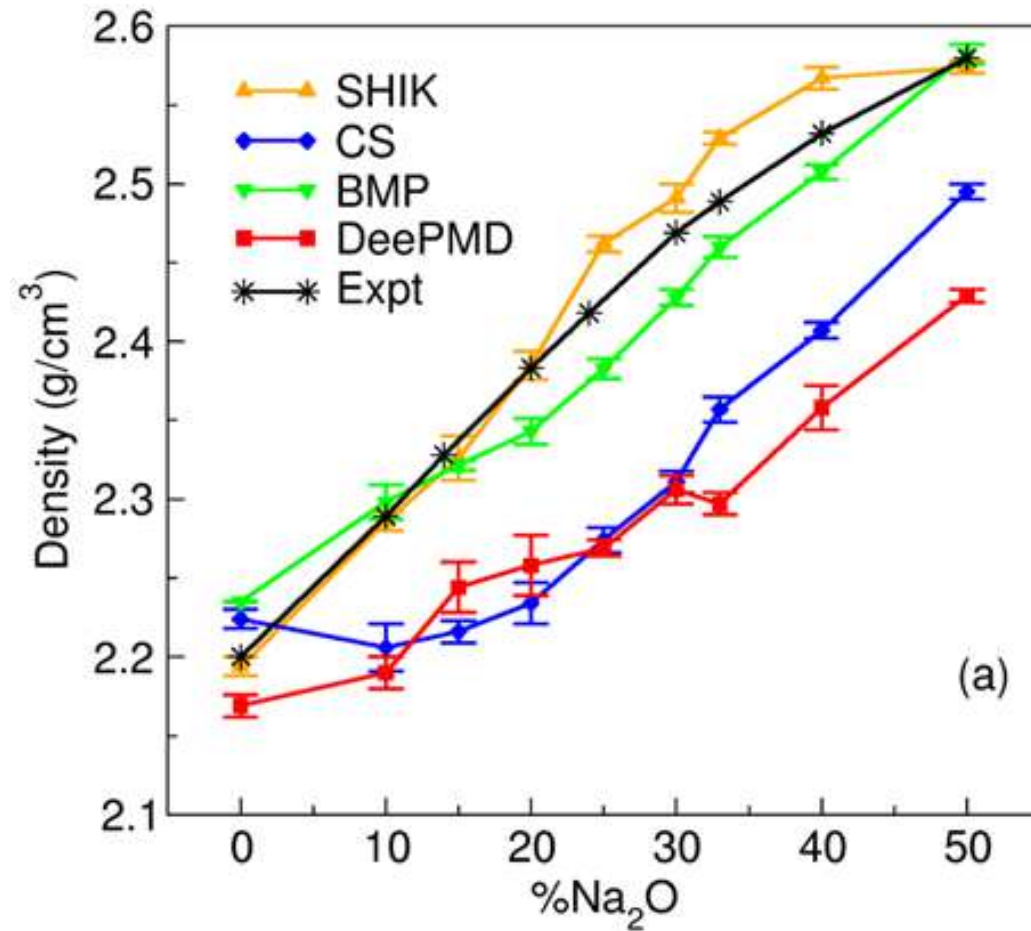
Coordination as a function of the oxidation state



Taken from Song et al. Advanced Functional Materials 28, 2018,1802564

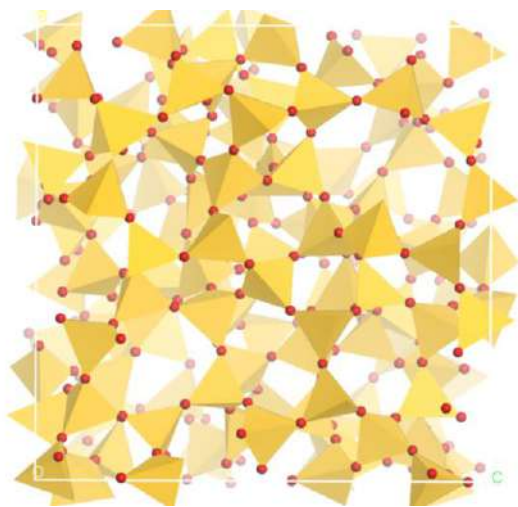
Wansi et al. JNCS 2023
<https://dx.doi.org/10.2139/ssrn.4570126>

Performance of Empirical and ML-potentials: Sodium Silicate Glasses

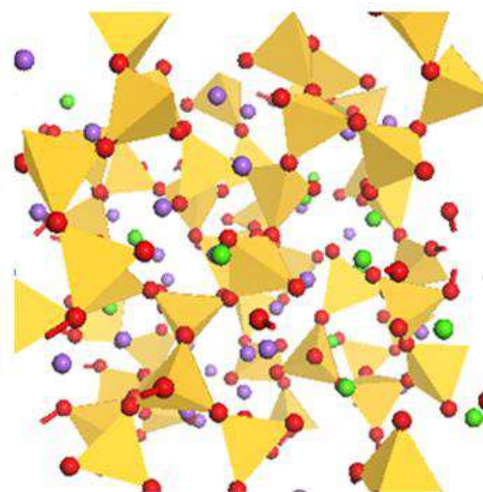


Total Distribution Functions and Bond Angle Distributions

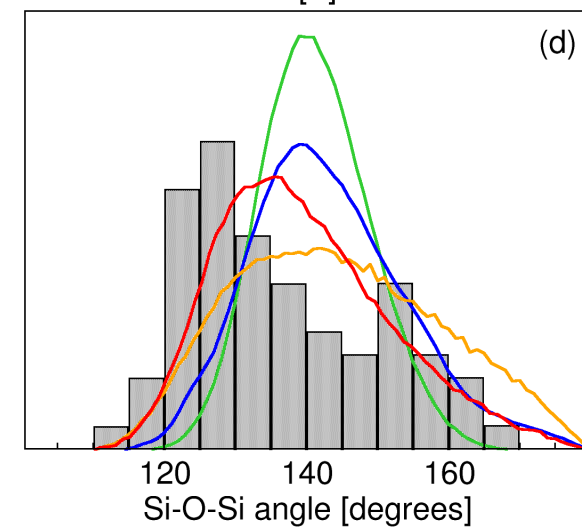
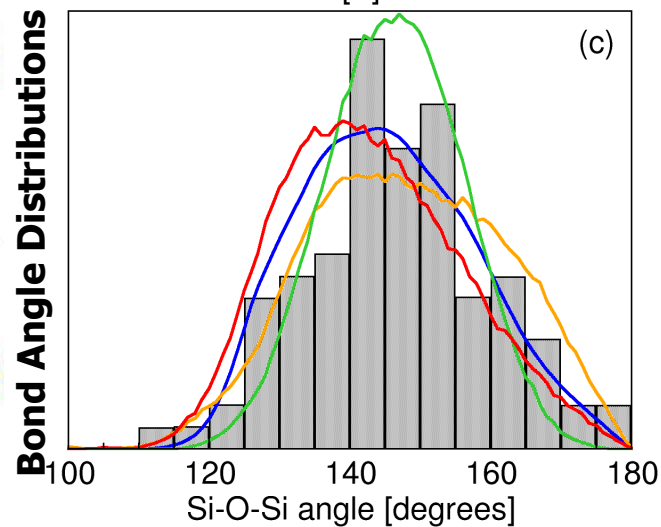
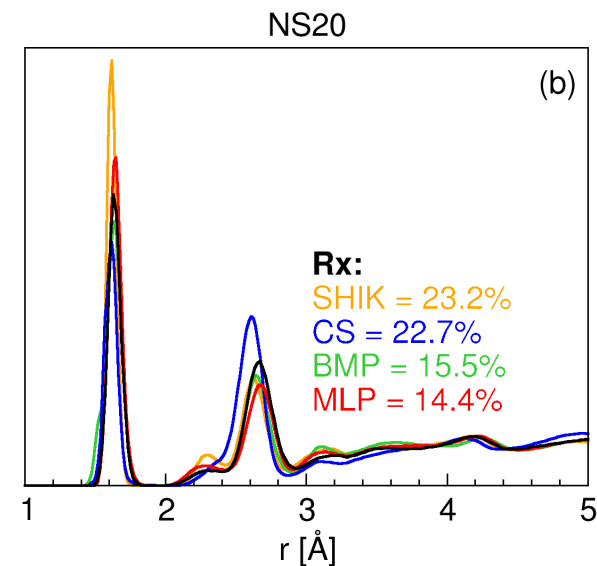
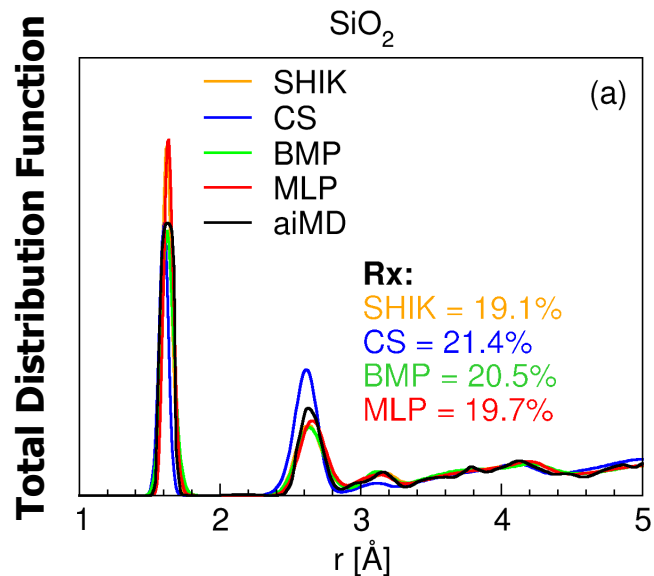
$$R_x = \left\{ \frac{\sum_{i=1}^N [T^{exp}(r_i) - T(r_i)]^2}{\sum_{i=1}^N [T^{exp}(r_i)]^2} \right\}^{\frac{1}{2}} \cdot 100$$



SiO₂

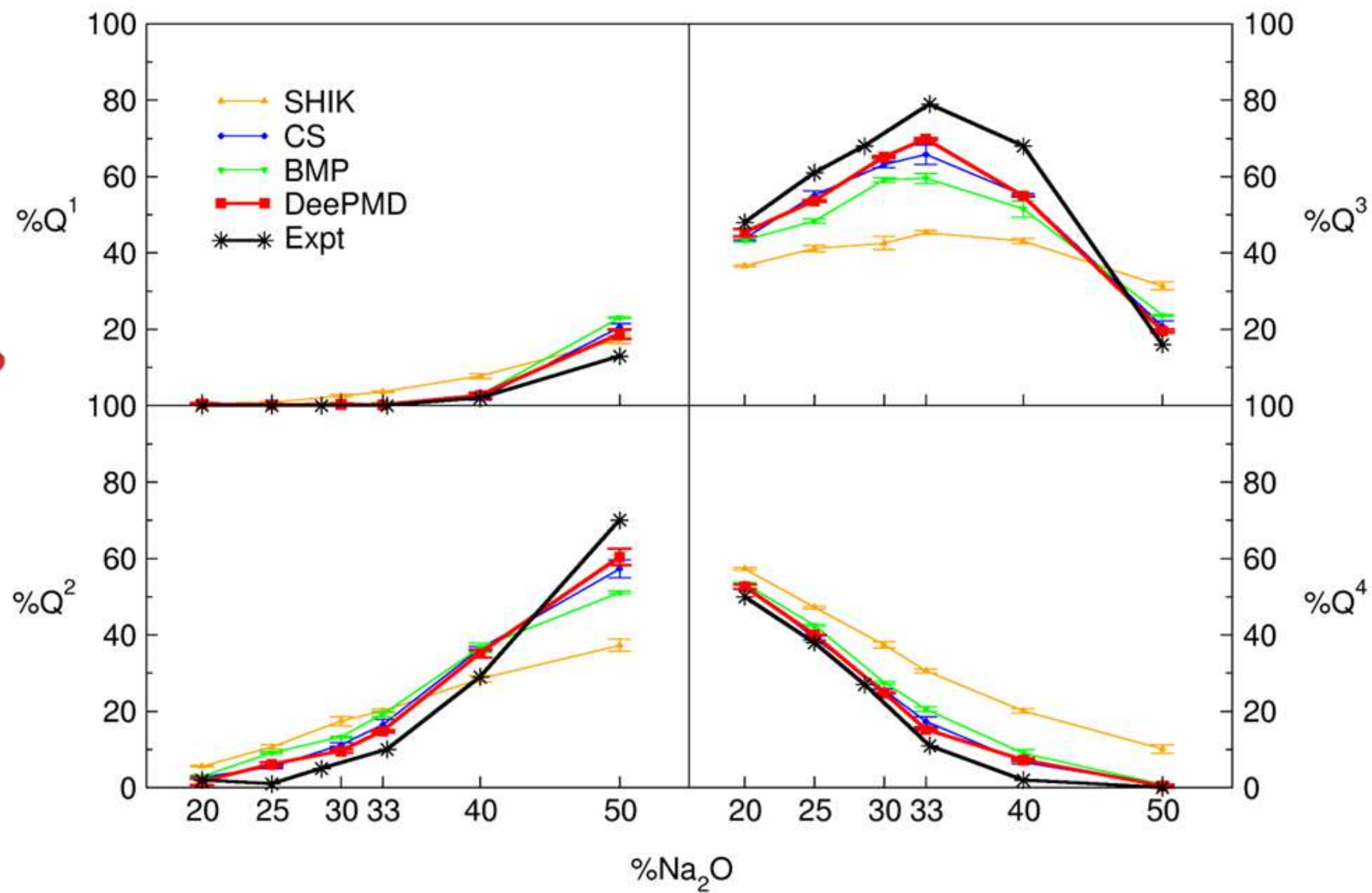
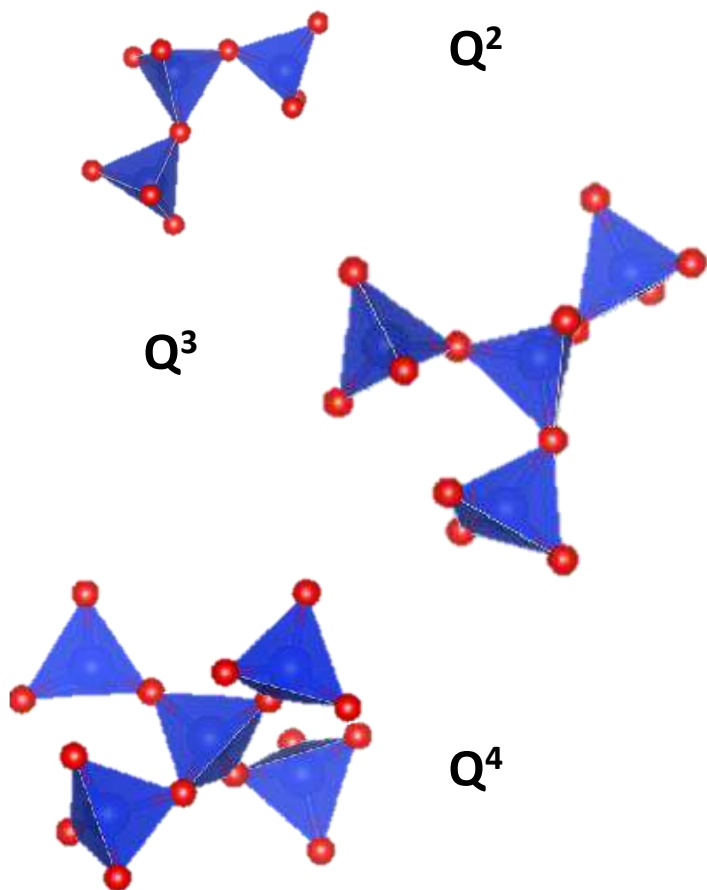


20Na₂O 80SiO₂

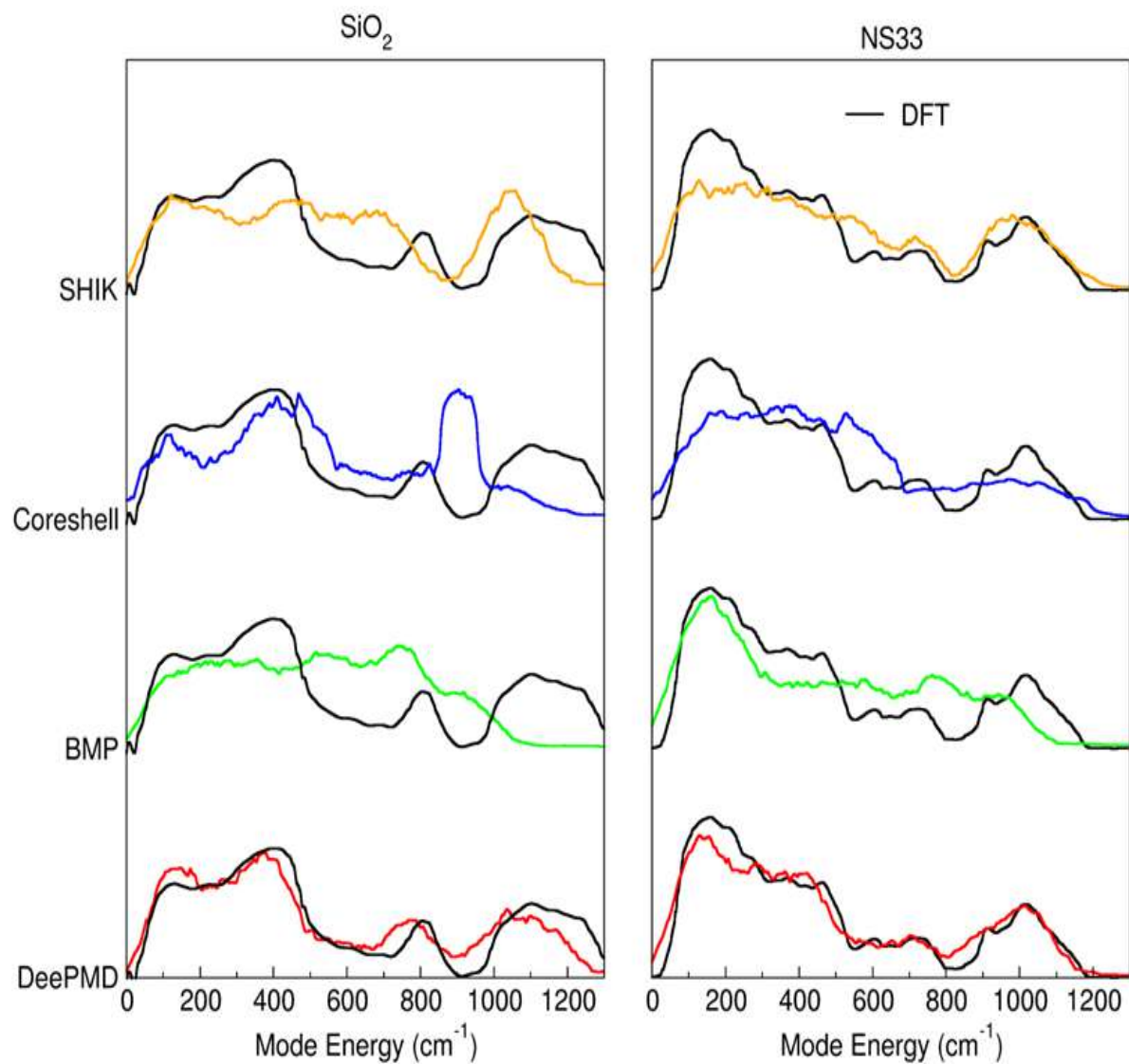


Qⁿ distributions

Si[Qⁿ] speciation

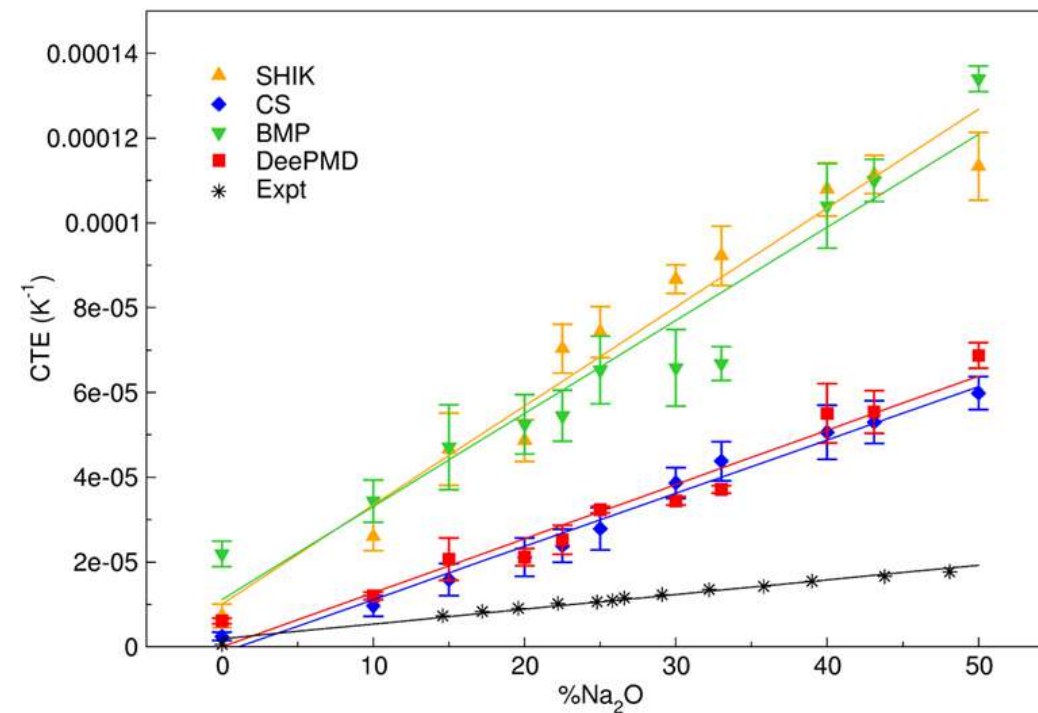


Vibration Density of States

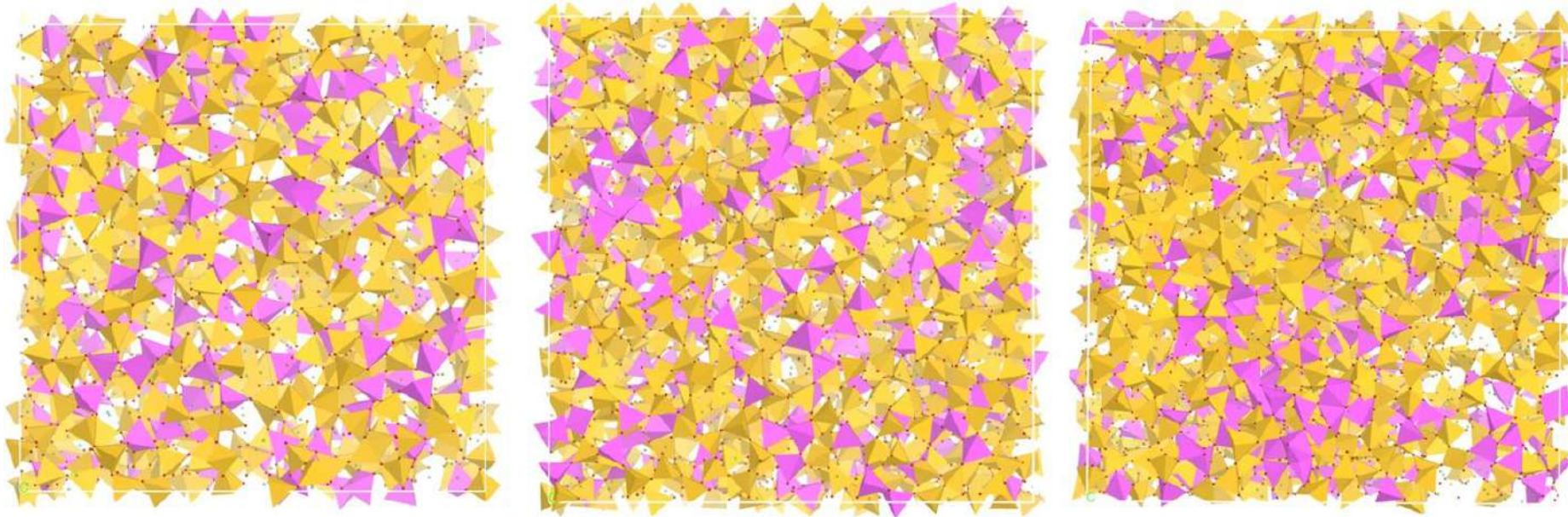


Coefficient of Thermal Expansion (CTE)

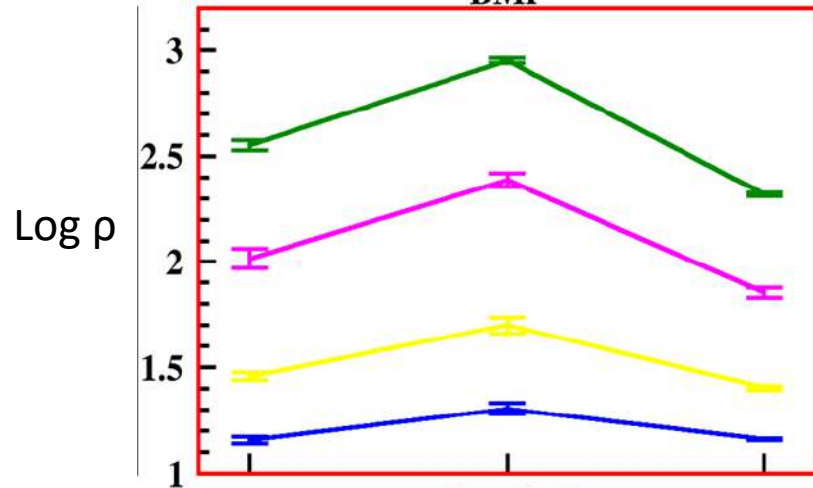
$$CTE = \frac{1}{V_0} \frac{dV}{dT}$$



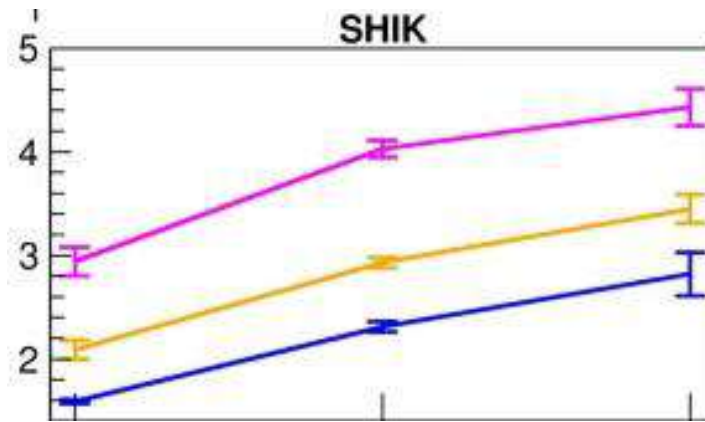
Mixed Alkali Effects (MAE) in AluminoSilicate Glasses not observed with all empirical FFs



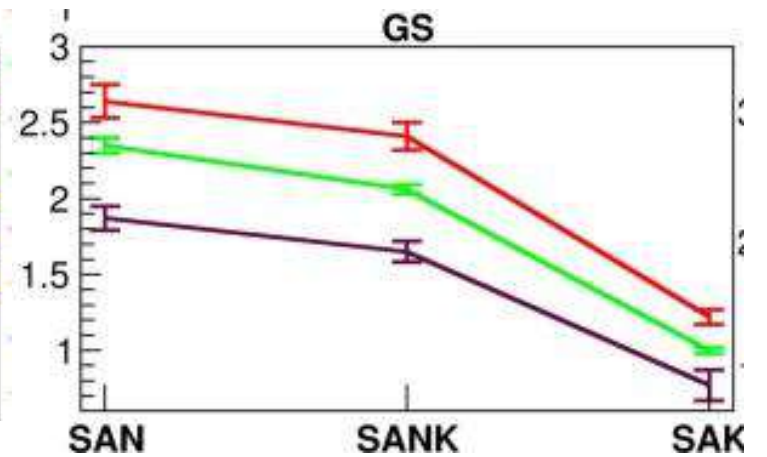
BMP



SHIK



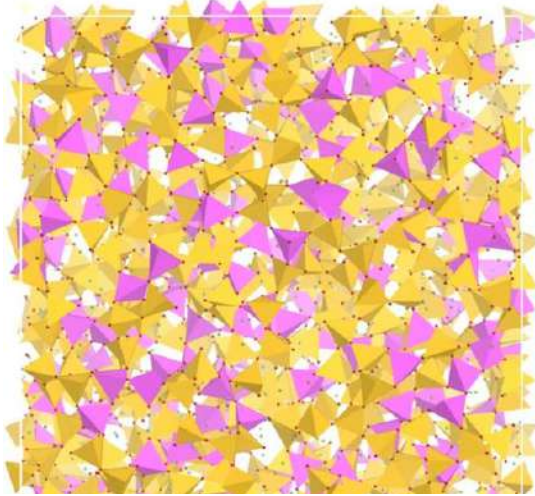
GS



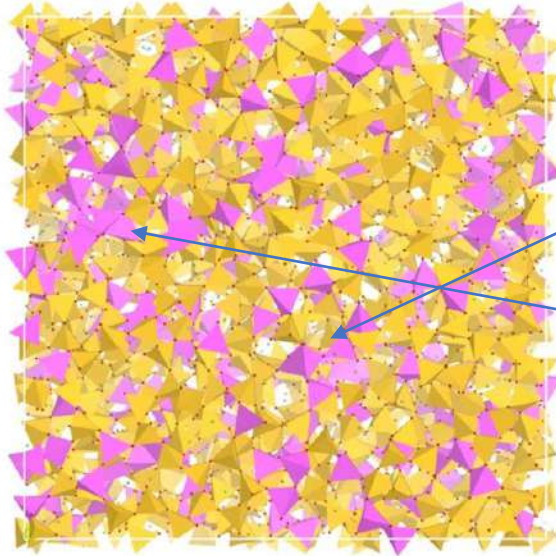
Wrong Structural Models – No Mixed Alkali Effect observed

... Effect of the structural models

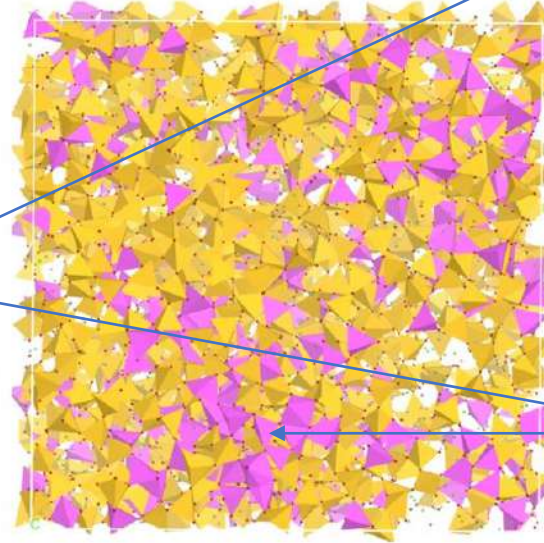
Clusterization



High Si-O-Al intermixing

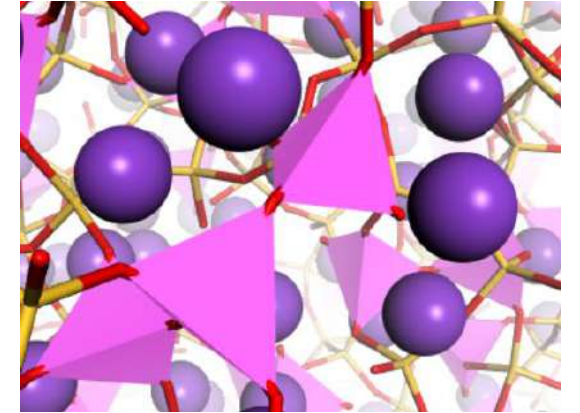


SHIK

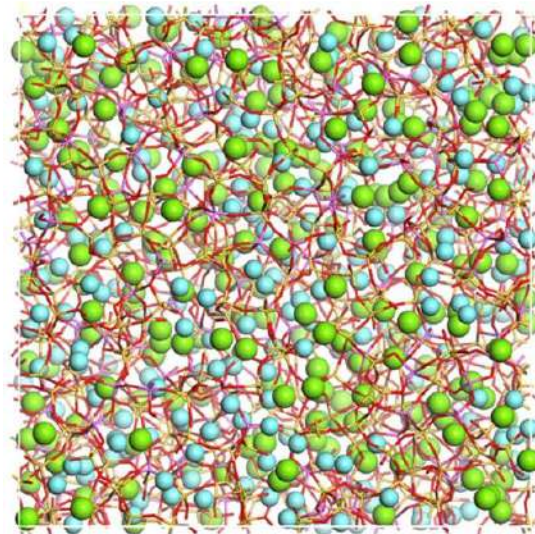


GS

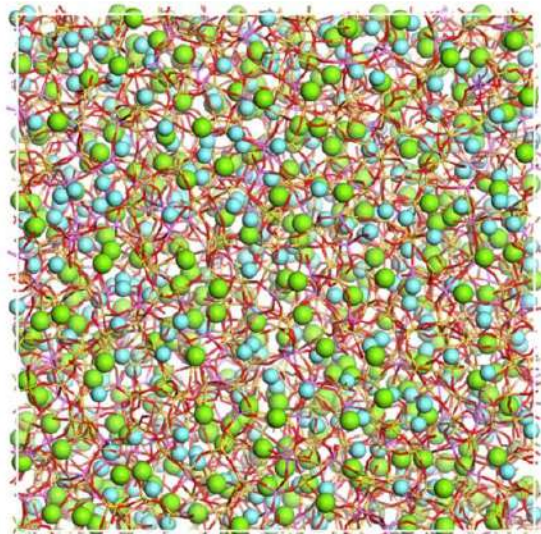
Strong Al-K interaction
Low K mobility



Al clusterization

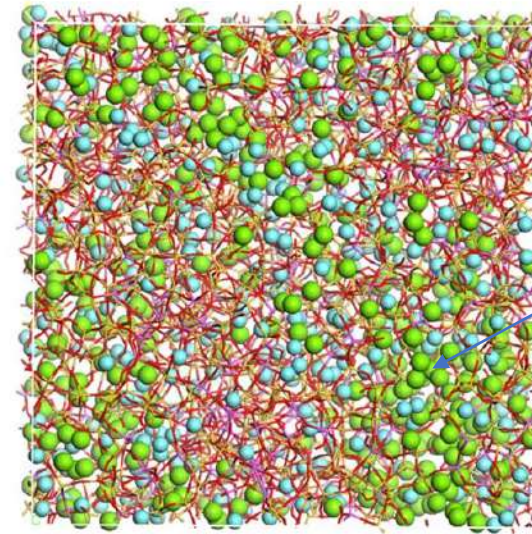


BMP

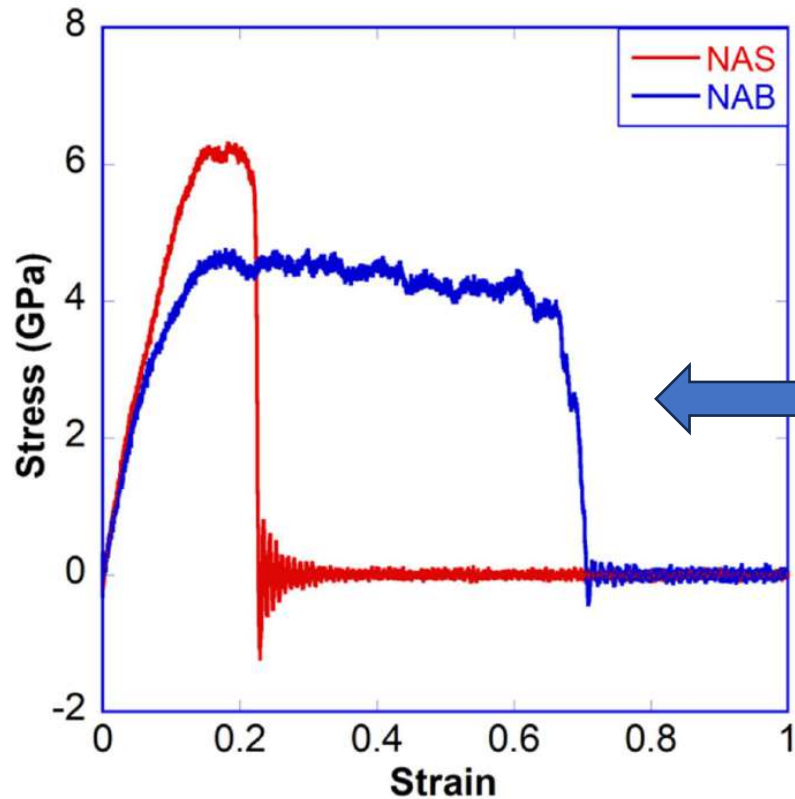


K clusterization

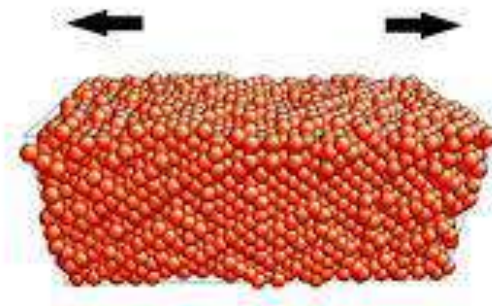
High K mobility



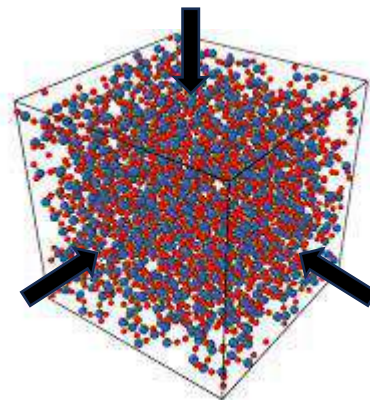
Mechanical Tests and Properties



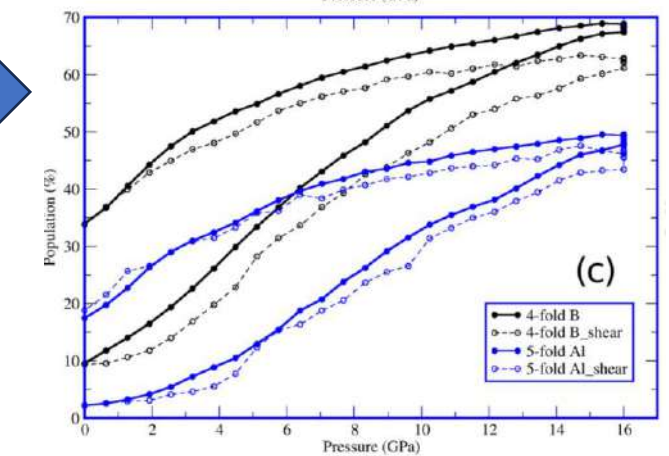
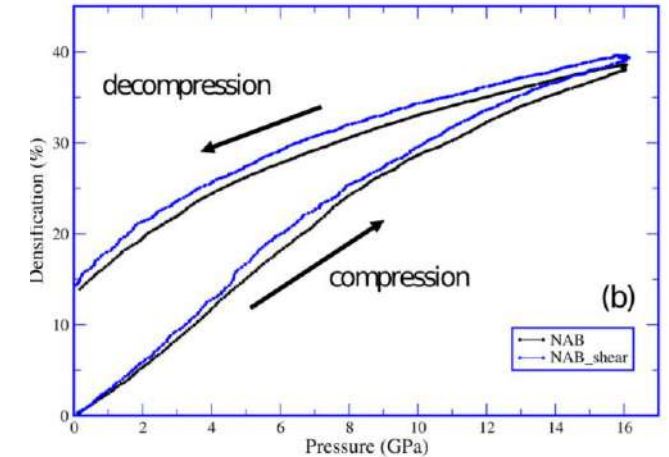
Elastic moduli, strength, fracture mechanisms



Uniaxial Tensile Tests

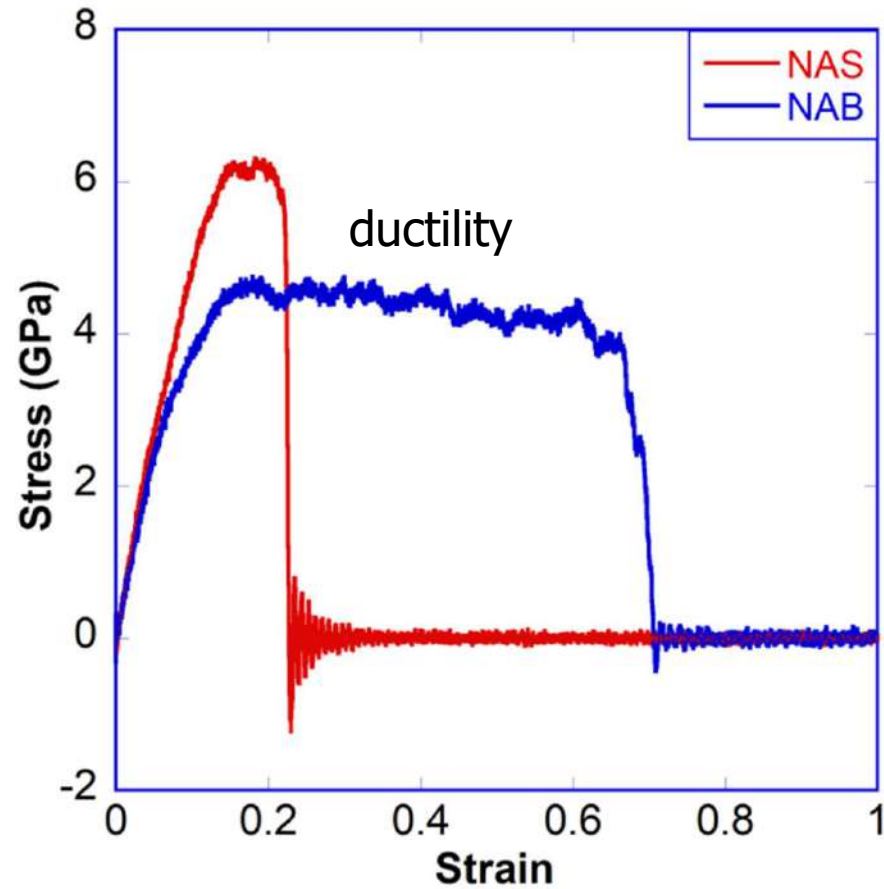


Hydrostatic Compressive Tests



Densification mechanism, bulk modulus

- NAB glasses more crack resistance than NAS
- NAB glasses show ductility compared to NAS
- Shear strain taken up by B in NAB glasses



Atomic Shear Strain

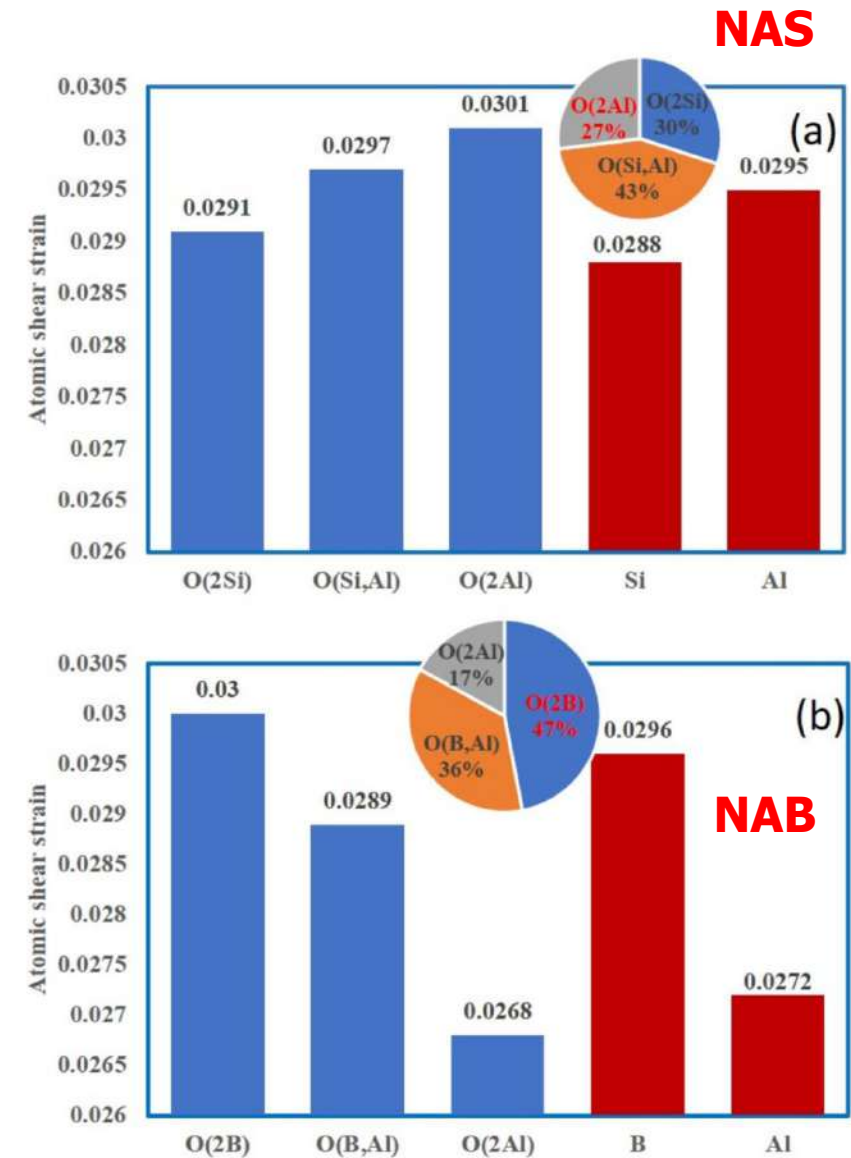


FIG. 6. Local shear deformation propensity in the NAS (a) and the NAB (b) at 300 K. Population of O with two neighbors of Si, Al, and B in different combinations are shown in the pie chart insets.

Indentation tests

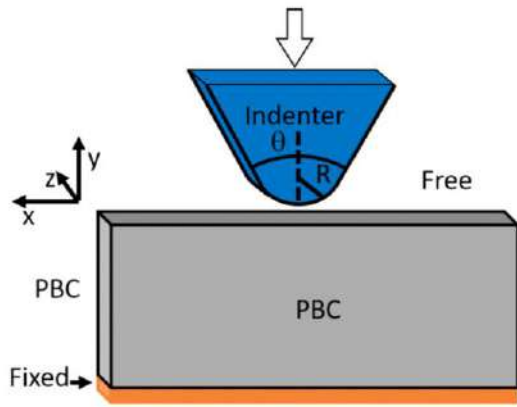
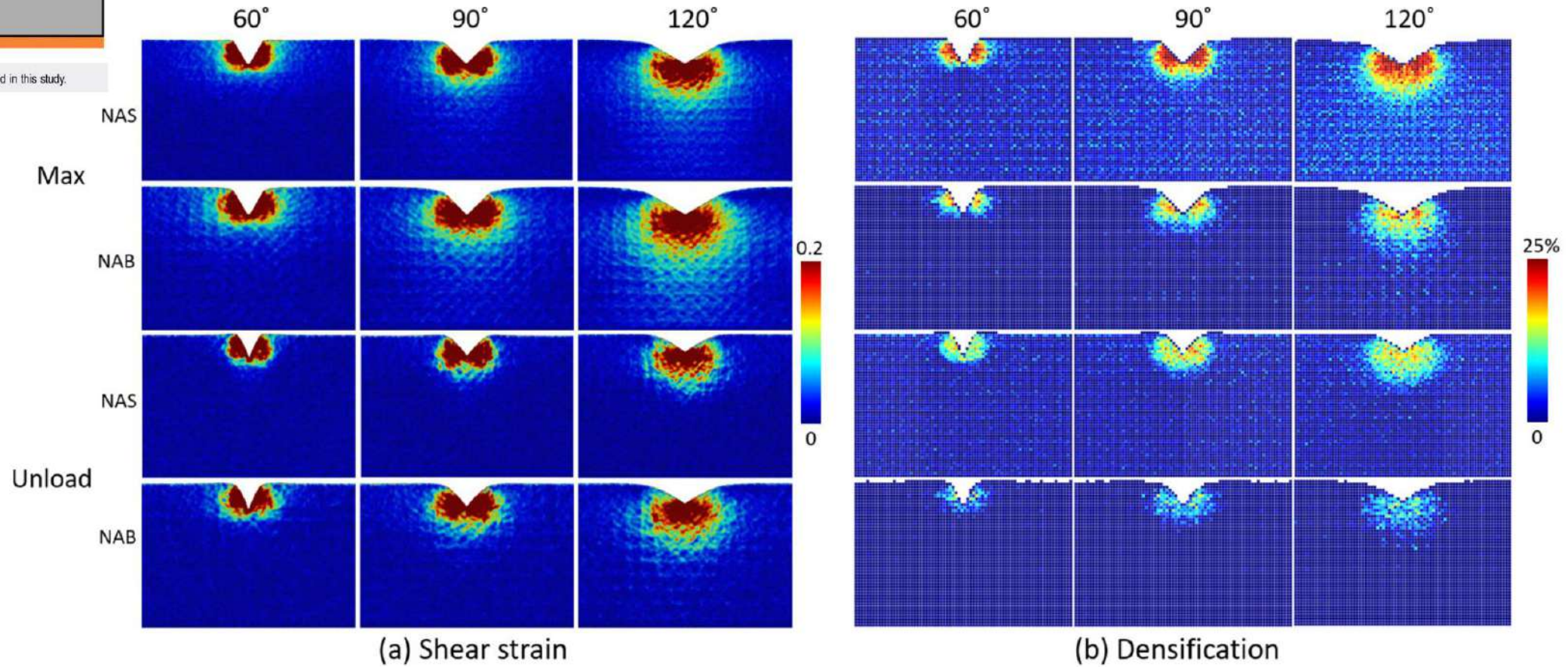


FIG. 1. Schematic of the nanoindentation setup used in this study.



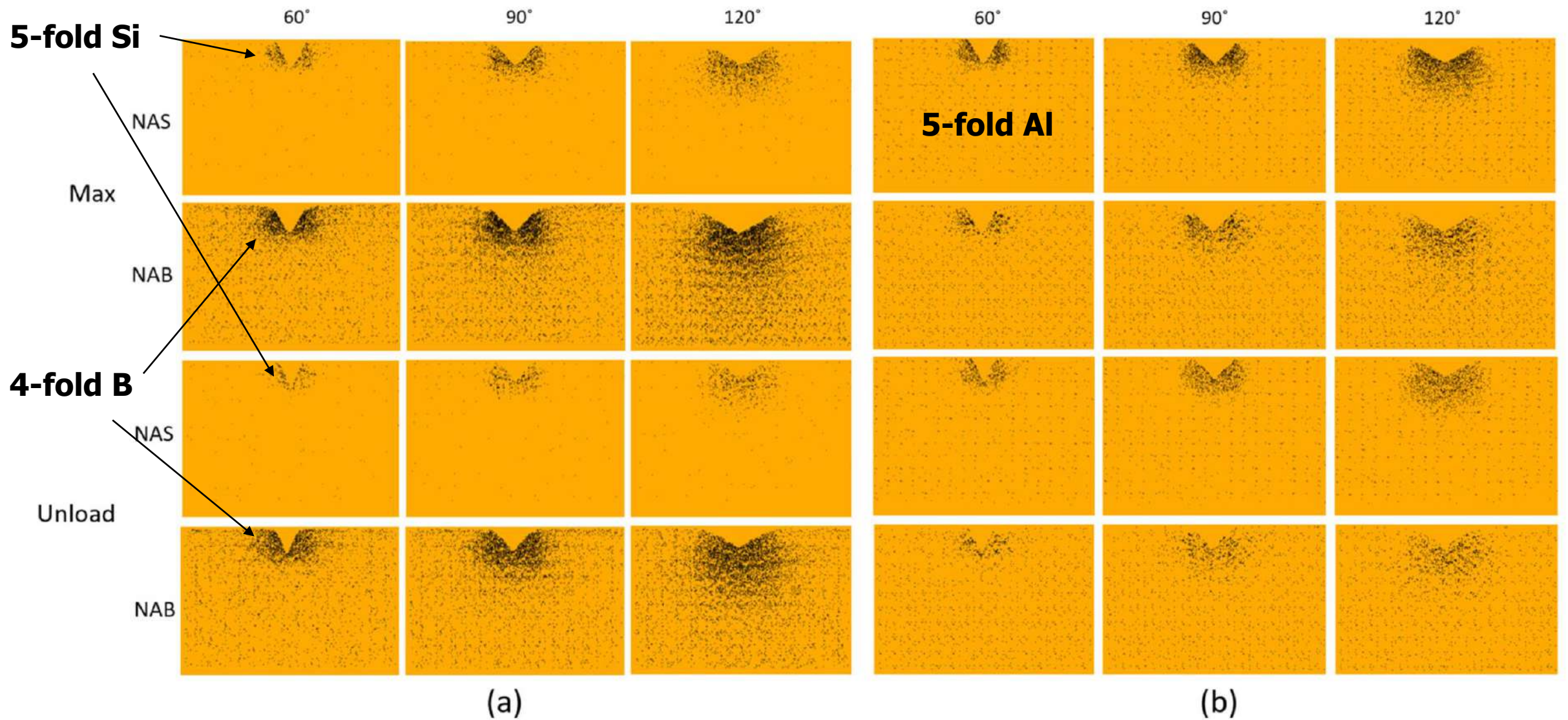


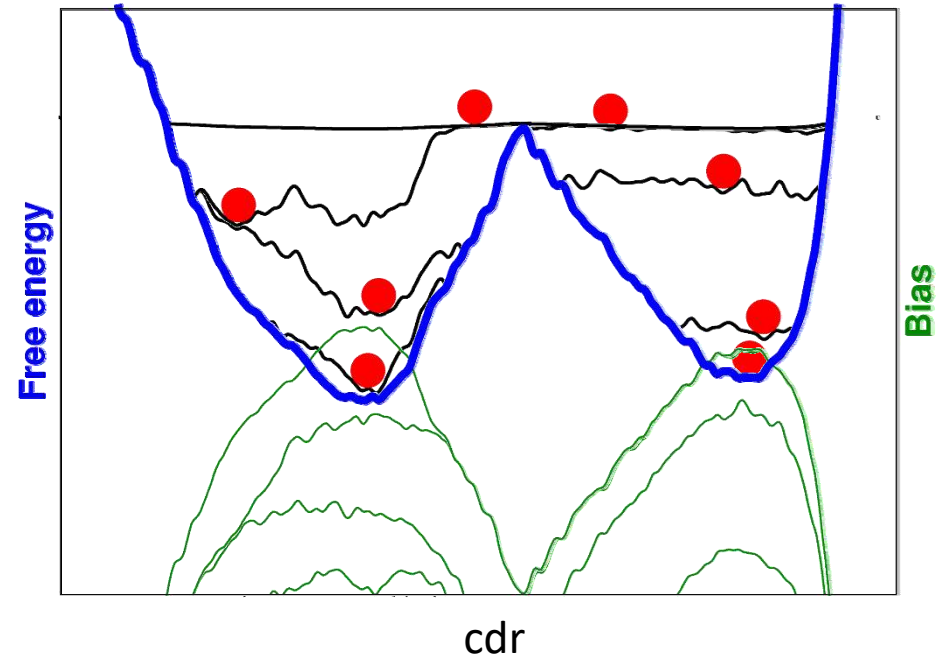
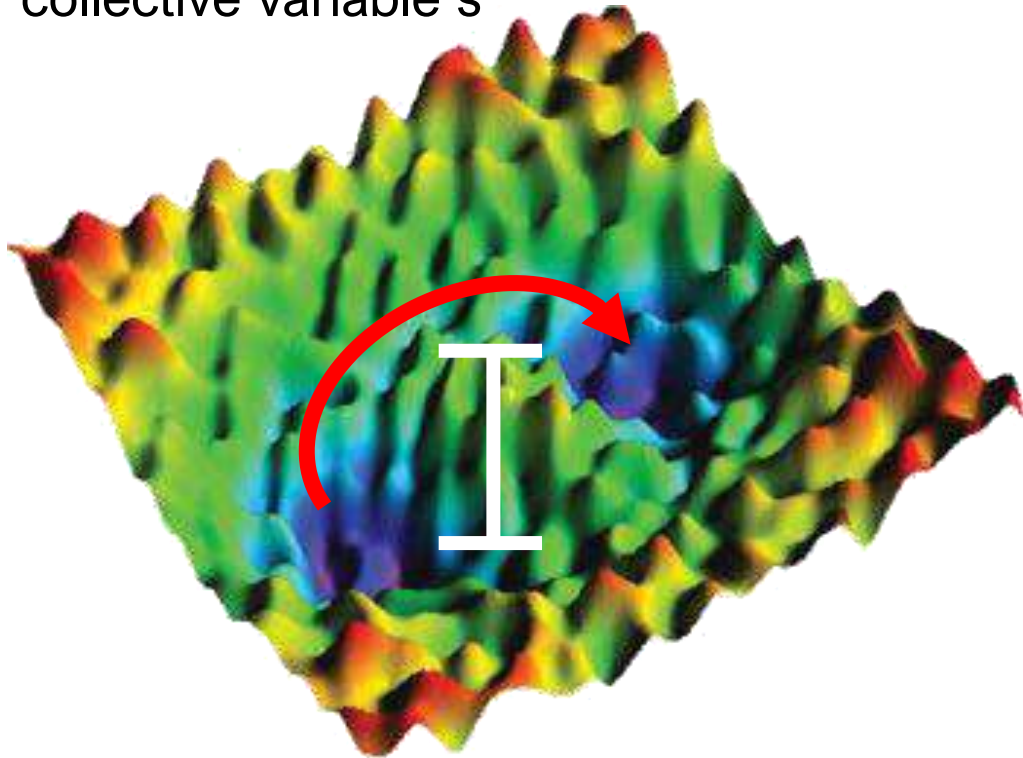
FIG. 12. (a) Distribution of fivefold coordinated Si atoms (indicated as black dots) in the NAS and fourfold coordinated B atoms (indicated as black dots) in the NAB at the maximum indentation depth (top two rows) and after unloading (bottom two rows) tested with different indenter angles (60°, 90°, and 120°) and a tip radius of 1 nm at 300 K. (b) Distribution of fivefold coordinated Al atoms (indicated as black dots) in the NAS and NAB at the maximum indentation depth (top two rows) and after unloading (bottom two rows) under the same indentation conditions.

Studying Crystallization in glasses: Metadynamics

- Enhanced Sampling Techniques

Add **bias potential** in the explored space along a collective variable s

$$U(\vec{r}) \rightarrow U(\vec{r}) + V_{BIAS}(s(\vec{r}))$$

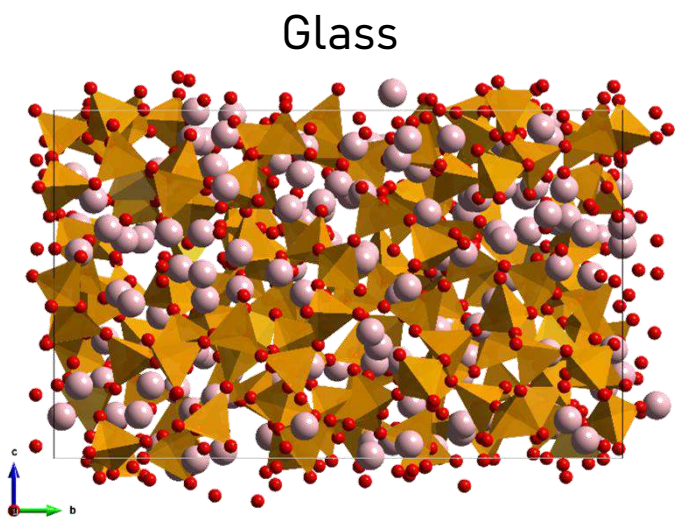
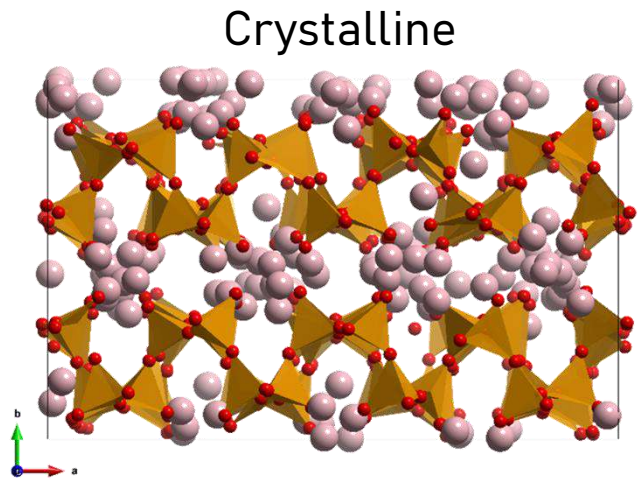


Reconstruct the **Free Energy Surface** (FES)

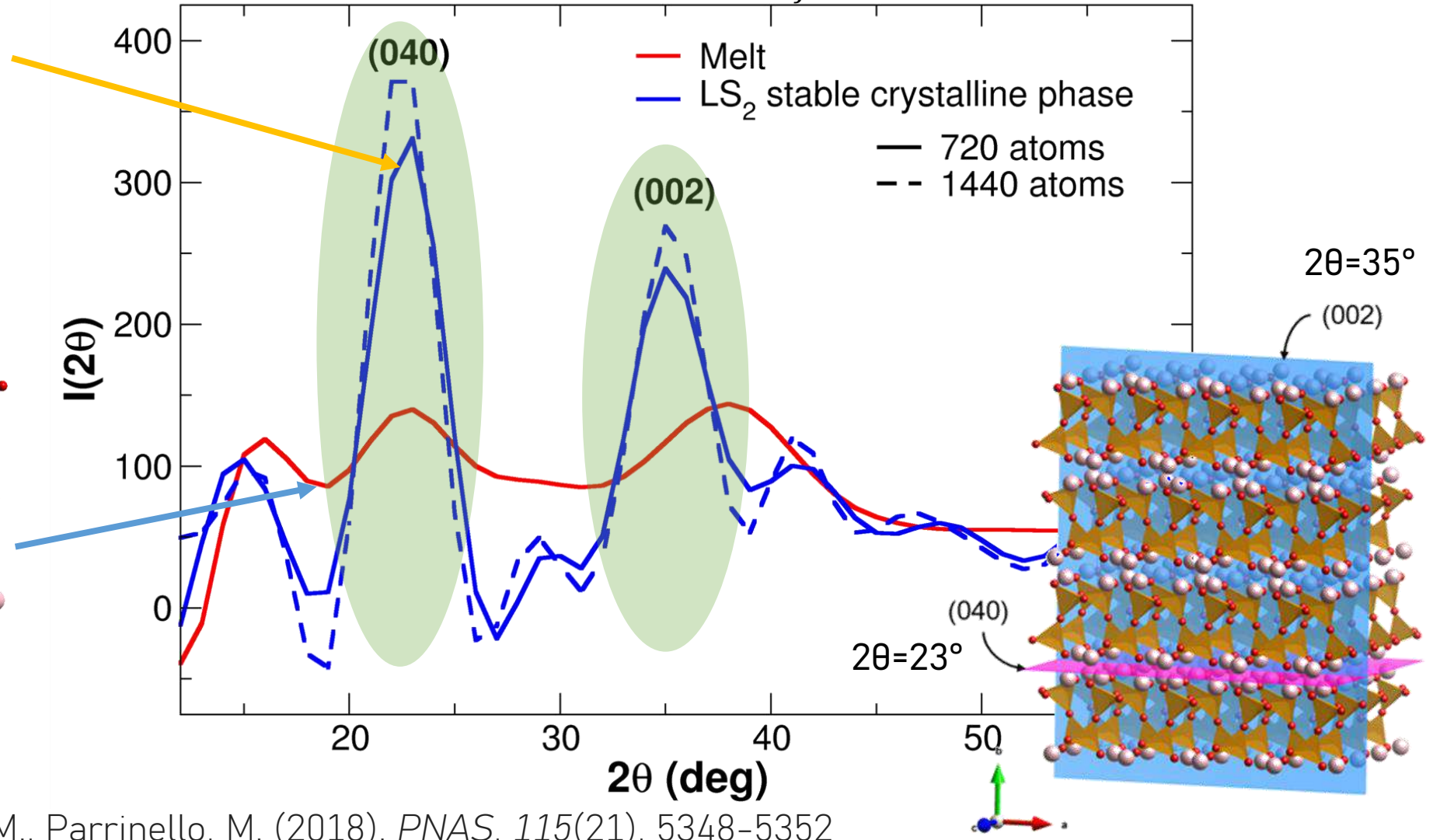
$$F(s) = -\frac{\gamma}{\gamma - 1} V(s, t) - c(t)$$

Lithium Disilicate

Collective Variable

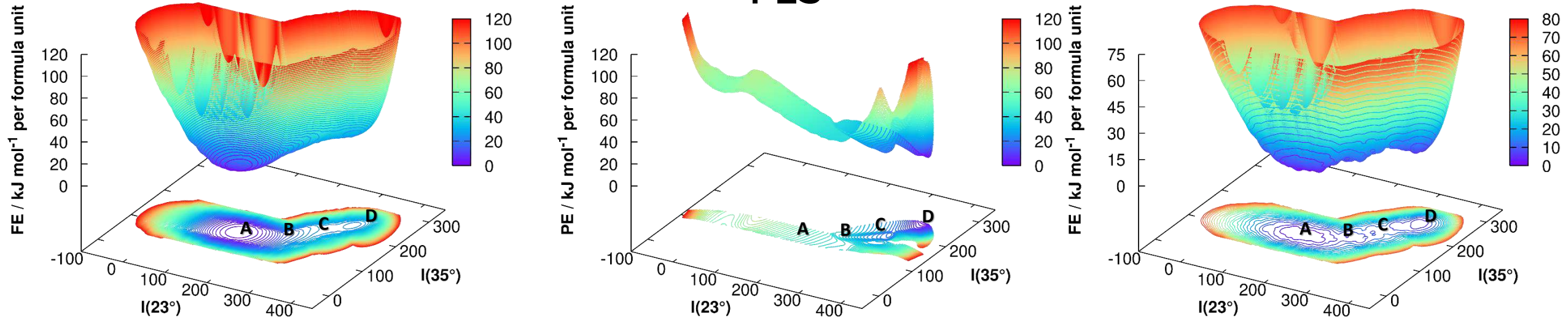


X-ray diffraction:
$$I(Q) = \frac{1}{N} \sum_{i=1}^N \sum_{j=1}^N f_i(Q) f_j(Q) \frac{\sin(Q \cdot R_{ij})}{Q \cdot R_{ij}} W(R_{ij})$$



Free Energy Surface of Lithium Disilicate Crystallization

PES

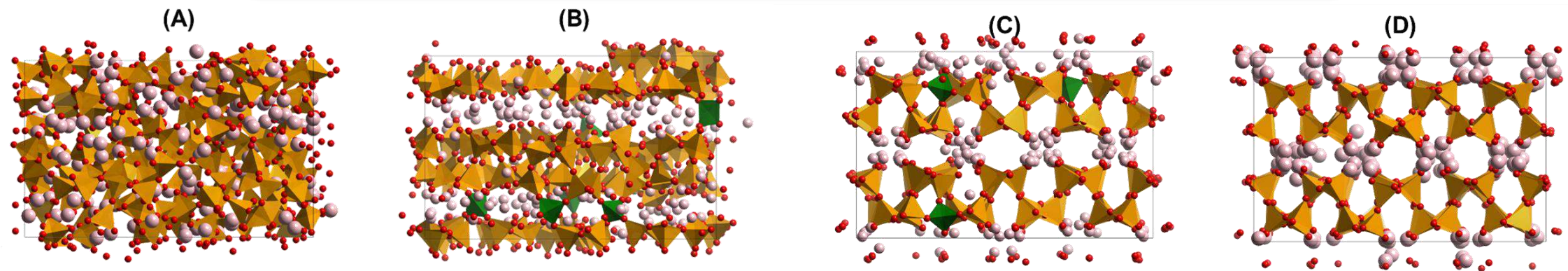


FES at 1800 K

Temperature rescaling

$$P_T(R, t) = P_{T'}(R) e^{-(\beta - \beta')H(R, t)}$$

FES at 1200 K



Step mechanism:

intermediate phase made of disordered layers

Conclusions

Molecular Dynamics Simulations allow to study the structure, properties and behaviour of multicomponent oxide glasses.

Some Challenges remain:

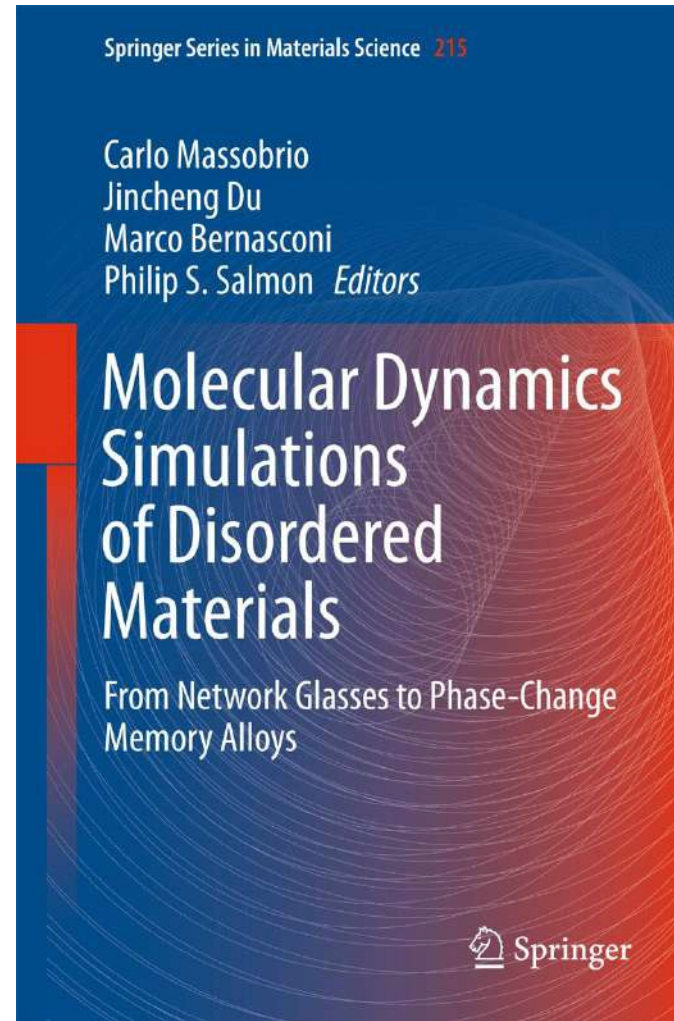
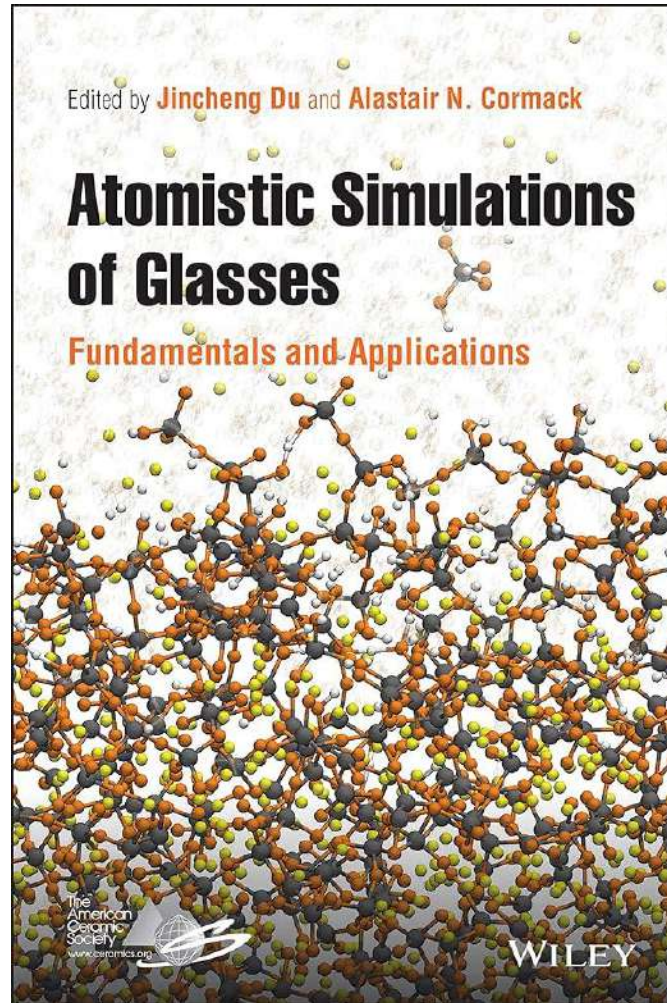
Developing accurate Force-Fields (machine learning and empirical)

Time scale problem (too high quenching rates)

Methods and protocols for simulation of properties

Reactivity for large systems and for long time

Books



Reviews

Pedone, A. *Properties Calculations of Silica-Based Glasses by Atomistic Simulations Techniques: A review.* **J. Phys. Chem. C**, (2009), 113, 20773-20784.
DOI:10.1021/jp9071263

Pedone, A.; Bertani, M.; Brugnoli, L.; Pallini, A. *Interatomic Potentials for oxide glasses: Past, present, and future.* **J. Non-Cryst. Solids: X** (2022) 15 100115.
<https://doi.org/10.1016/j.nocx.2022.100115>

Urata, S.; Bertani, M.; **Pedone, A.** *Applications of Machine-Learning Interatomic Potentials for modeling Ceramics, Glass, and Electrolytes; a review.* **J. Am. Cer. Soc.** (2024)

Acknowledgments

Collaborators

Dr. Thibault Charpentier (Center for Atomic Energy, France)
Prof. Francesco Faglioni (UniMORE)
Dr. Marco Bertani (UniMORE)
Dr. Luca Brugnoli (UniMORE)
Dr. Federica Lodesani (UniMORE)
Dr. Annalisa Pallini (UniMORE)
Prof.ssa Maria Cristina Menziani (UniMORE)
Dr. Shingo Urata (AGC)
Dr. Wolfgang Mannstadt (SCHOTT)



2 NVIDIA Academic Grants



Ashai Glass Company, Japan



Thank you all for your attention!